Brain Structure and Function (2020) 225:481–510
https://doi.org/10.1007/s00429-019-02015-3

ORIGINAL ARTICLE

Longitudinal developmental analysis of prethalamic eminence derivatives in the chick by mapping of Tbr1 in situ expression

Antonia Alonso[1,2] · **Carmen María Trujillo**[3] · **Luis Puelles**[1,2]

Received: 11 May 2019 / Accepted: 12 August 2019 / Published online: 4 January 2020

Abstract

The prethalamic eminence (PThE) is the most dorsal subdomain of the prethalamus, which corresponds to prosomere 3 (p3) in the prosomeric model for vertebrate forebrain development. In mammalian and avian embryos, the PThE can be delimited from other prethalamic areas by its lack of *Dlx* gene expression, as well as by its expression of glutamatergic-related genes such as *Pax6*, *Tbr2* and *Tbr1*. Several studies in mouse embryos postulate the PThE as a source of migratory neurons that populate given telencephalic centers. Concerning the avian PThE, it is visible at early embryonic stages as a compact primordium, but its morphology becomes cryptic at perinatal stages, so that its developmental course and fate are largely unknown. In this report, we characterize in detail the ontogeny of the chicken PThE from 5 to 15 days of development, according to morphological criteria, and using *Tbr1* as a molecular marker for this structure and its migratory cells. We show that initially the PThE contacts rostrally the medial pallium, the pallial amygdala and the paraventricular hypothalamic alar domain. Approximately from embryonic day 6 onwards, the PThE becomes progressively reduced in size and cell content due to massive tangential migration of many of its neuronal derivatives towards nearby subpallial and hypothalamic regions. Our analysis supports that these migratory neurons from the avian PThE target telencephalic centers such as the commissural septal nuclei, as previously described in mammals, but also the diagonal band and preoptic areas, and hypothalamic structures in the paraventricular hypothalamic area.

Keywords Thalamic eminence · Neuronal tangential migration · Septum · Subpallium · Preoptic area · Diagonal band · Diencephalon

Abbreviations

ac	Anterior commissure
AC	Nucleus of anterior commissure
ACo	Amygdala, core nucleus
ah	Amygdalohypothalamic tract
AHi	Amygdalohippocampal area
AHil	Amygdala, hilar region
ATn	Amygdalar taenial nucleus
BSM	Bed nucleus of the stria medullaris
ComSe	Commissural septum
csm	Cortico-septo-mesencephalic tract
CoS	Commissural septal nucleus
CoSM	Commissural septal nucleus medial part
CoSL	Commissural septal nucleus lateral part
cht	Chorioidal tela
DB	Diagonal band nuclei
Dg	Diagonal band area
EA	Subpallial extended amygdala
ech	Eminential chorioidal tela
EPD	Dorsal entopeduncular nucleus
ESA	Eminentio-septal area
EW	Eminential wings
fi	Fimbria
fich	Telencephalic fimbrial chorioidal tela
Hb	Habenula
HDB	Horizontal limb of the diagonal band
Hi	Hippocampus
hic	Hippocampal commissure

✉ Antonia Alonso
antoniaaf@um.es

[1] Department of Human Anatomy and Psychobiology, Faculty of Medicine, School of Medicine, University of Murcia, 30100 Murcia, Spain

[2] Biomedical Research Institute of Murcia Region, Laboratory of Biomedical Research (LAIB), Campus of Health, El Palmar, 30120 Murcia, Spain

[3] Department of Biochemistry, Microbiology, Cell Biology and Genetic, Faculty of Sciences, School of Biology, University of La Laguna, 38200 Canary Islands, Spain

HiC	Hippocampal commissure nucleus
ivf	Interventricular foramen
IIIv	Third ventricle
LH	Lateral hypothalamus
LPO	Lateral preoptic area
LTer	Lamina terminalis
lv	Lateral ventricle
MA	Medial amygdala
MPO	Medial preoptic nucleus
MnPO	Paramedian preoptic nucleus
MPall	Medial pallium
NCM	Nidopallium, caudal part, medial region
oc	Optic chiasm
Pa	Paraventricular nucleus
Pal	Pallidus
Pall	Pallium
PallA	Pallial amygdala
PallSe	Pallial septum
pe	Cerebral peduncle
PHy	Peduncular hypothalamus
Pir	Piriform cortex
POA	Preoptic area
POI	Preoptic island
POM	Medial preoptic area
PTh	Prethalamus
PThE	Prethalamic eminence
Se	Septum
SFi	Septofimbrial nucleus
sm	Stria medullaris tract
SO	Supraoptic nucleus
soc	Supraoptic commissure
SPall	Subpallium
St	Striatum
svz	Subventricular zone
Th	Thalamus
thch	Thalamic chorioidal tela
ts	Terminal sulcus
TS	Triangular septal nucleus
TP	Temporal pole
Tu	Olfactory tubercle
THy	Terminal hypothalamus
vaf	Ventral amygdalofugal tract
VDB	Vertical limb of the diagonal area
VPall	Ventral pallium
vz	Ventricular zone
zl	Zona limitans interthalamica

Introduction

The prethalamic eminence (PThE; often misidentified in the literature as 'thalamic eminence') is an obscure diencephalic region limiting with the telencephalo-hypothalamic border zone and stria terminalis domain. It is best known as related to the course of the stria medullaris tract, forming its diencephalic bed nucleus (BSM), before it enters the habenular thalamic region; note there are other populations interstitial to the stria medullaris within the hypothalamus (Puelles et al. 2012). Several embryologic studies and atlases identify the PThE at early-middle developmental stages, but it becomes indistinct at later stages, so that it is not identified in most adult brain atlases (an exception is the chick brain atlas; Puelles et al. 2007, 2019).

The present systematization of PThE developmental changes in the chicken was intended to aid instrumentally the interpretation of fate-mapping quail–chick homotopic grafts we had performed before, whose results will be interpreted in a companion paper using our present anatomic conclusions.

We accordingly present here mainly a longitudinal descriptive analysis of the late-embryonic chicken prethalamic eminence (PThE) based on in situ *Tbr1* mRNA mappings. This work aims to follow in detail the apparent developmental fate of the eminential *Tbr1*-positive primordium into its obscure final status. Indeed, its population results progressively reduced, though not totally, apparently due to tangential migration of various neuronal derivatives to neighbouring or distant targets within the secondary prosencephalon (hypothalamus plus telencephalon). Given the descriptive nature of our present approach, all reference made here to migrations is hypothetic (based on objective histological images suggesting displacements of specific labelled cell populations), pending our publication of corroborating experimental evidence.

Within the updated prosomeric forebrain model (Puelles et al. 2012; Puelles and Rubenstein 2015; Puelles 2018) the PThE is an alar subdomain of the diencephalic prethalamus (prosomere 3; p3), found along the dorsalmost alar position, next to the taenial attachment of the local chorioidal roof plate. This p3 subdomain can be readily delimited molecularly from more ventral prethalamic alar areas by its exclusive lack of *Dlx* family gene expression, and characteristic ventricular or mantle expression, among others markers, of *Pax6*, *Tbr2*, *Tbr1*, *Lhx5*, *Lhx9*, and *Calb2* (Shimogori et al. 2010; Puelles et al. 2012). This molecular profile allows the PThE to be distinguished from neighbouring thalamic, telencephalic and hypothalamic areas, irrespective of partial sharing of some of these markers with one or more of the neighbouring forebrain territories. The PThE lies strictly rostral to the similarly hyperdorsal habenular region of the thalamus (p2). In fact, as mentioned above, both areas are sequentially traversed longitudinally by the stria medullaris tract, which starts within the telencephalo-hypothalamic boundary region, crosses longitudinally the whole PThE (p3), and ends at the habenula, or enters the habenular commissure (p2).

The avian PThE (like its mammalian homolog; Puelles et al. 2019) is partly co-evaginated into the posteromedial wall of the telencephalon, where it meets the hippocampus under the chorioidal fissure. As a consequence, part of its ventricular surface is observed at the caudal aspect of the interventricular foramen, where it bends backwards, extending into the posterior bank of the terminal sulcus. Such eminential evagination is less marked in the chick than in mammals (Bardet 2007; Bardet et al. 2008; present data). The ventricular bulge of the bent PThE at the back of the foramen justifies its traditional description as an 'eminence'. Before the discovery within neuromeric forebrain models of the prethalamic diencephalic alar sector (see historic accounts in Puelles 2018, 2019), it used to be wrongly assumed that this eminence was 'thalamic', habitually joining the equally wrong idea that the thalamus here contacts the 'corpus striatum' (meaning what we now understand as a prethalamic relationship with the pallido-diagonal medial ganglionic eminence; Puelles 2019; see also Puelles et al. 2013, 2016a, b). The classic hemispheric sulcus, which as a result of this partial evagination indents the eminential pial surface, was held to divide the telencephalon from the diencephalon (e.g., Johnston 1909; Kuhlenbeck 1973), but is actually an inaccurate external landmark that is not consistent with the true molecular diencephalo(prethalamo)-telencephalic boundary.

The dorsoventral dimension of the PThE expands rostrally, probably because it participates in the mitogenic stimulus that expands the telencephalic field. This allows it to contact via its topologically dorsal postforaminal evaginated portion [see use of this term in Puelles (2019)] the caudal end of the medial pallium (hippocampus) and the underlying pallial amygdala, while its topologically ventral part meets the paraventricular hypothalamic alar domain under the foramen and along the ascending vertical spike of this area that also evaginates jointly along the hypothalamo-diencephalic border (Fig. 1a; Fan et al. 1996; Puelles et al. 2000, 2012; Puelles and Rubenstein 2003, 2015).

The avian PThE is clearly visible at early and middle embryonic stages, but becomes rather cryptic at perinatal or postnatal stages, unless mapped with PThE-specific molecular markers. As mentioned above, the characteristic markers of the PThE include *Calb2*, *Lhx9*, *Lhx5*, *Tbr1*, *Tbr2* and *Pax6* (the latter two markers are expressed selectively in the ventricular PThE territory, as occurs in the telencephalic pallium; *Tbr1* is expressed widely and strongly in the PThE mantle layer, likewise as in the pallium; Puelles et al. 2000). This expression profile distinguishes the PThE from the rest of alar prethalamic territories, where genes such as *Dlx2/5/6, Six3,* and *Pax6* expressed in the mantle layer are characteristic (Puelles et al. 2000, 2012; Shimogori et al. 2010). On the other hand, the PThE shares with the hypothalamic paraventricular area (Pa) expression of *Pax6*, *Calb1*, *Tbr1* and *Fezf2* genes, thus defining jointly what is occasionally mentioned in the literature as the mixed (hypothalamo-prethalamic) 'optoeminential domain' (Bulfone et al. 1993, 1995; Puelles et al. 2012). Nevertheless, the Pa differentially expresses characteristic gene markers that are essentially absent at the PThE, including *Otp* and *Sim1/2* (Bardet 2007; Bardet et al. 2008; Puelles et al. 2012). As mentioned, the intrinsic PThE cell population forms basically a glutamatergic bed nucleus of the stria medullaris, which receives afferents from that tract, and also projects its own axons via the same pathway into the thalamic habenular region (Díaz and Puelles 1992a, b). The stria medullaris tract and the BSM were classically

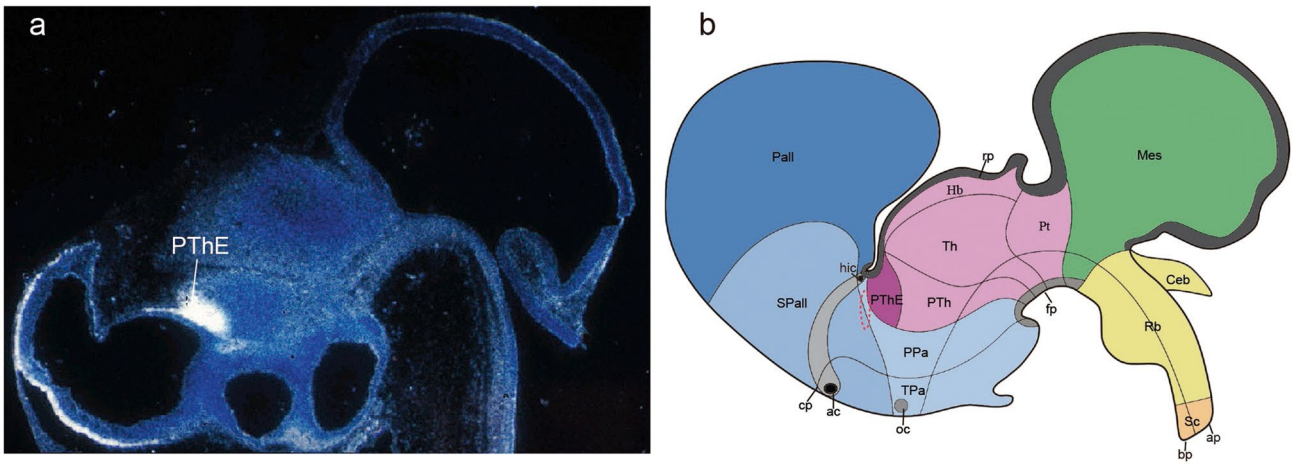

Fig. 1 *Tbr1* expression in the prethalamic eminence (PThE). **a** Microphotograph of a sagittal brain section from a HH26 chick embryo, processed for ISH with the *Tbr1* probe as commented in Methods, showing the expression of this gene in the PThE. Note its relationship with the interventricular foramen. **b** Schematic sagittal representation of the same section, showing the topological position of the PThE in relation to other forebrain structures. Note in particular the vicinity of PThE to pallium, hypothalamus and subpallium. The foramen of Monro is represented by a red dashed oval

conjectured to convey olfactory input to the habenula, apparently an error due to a postamygdalar component of the lateral olfactory tract which ascends through this pathway to a crossing in the habenular commissure, without any local habenular connections (but some secondary olfactory fibres reach the underlying dorsomedial nucleus of the thalamus). Recent studies have established the stria medullaris as part of a striatal pathway involving the dorsal entopeduncular nucleus and targeting selectively the lateral habenula (Wallace et al. 2017). Other parallel pathways targeting the medial habenula are thus possible.

As development advances there apparently emerge from the PThE several neuronal migrating streams expressing eminential mantle markers, which penetrate the extended amygdala (EA), subpallial diagonal (Dg) and preoptic (POA) domains, as well as the whole septal commissural plate (next to anterior and hippocampal commissures), and the paraventricular hypothalamic area. This suggests their possible tangentially migrated eminential origin, though in some cases alternative migratory origins from pallial territories that express the same markers need to be considered (Bulfone et al. 1995, 1999; Puelles et al. 2000; Englund et al. 2005; El Mestikawy et al. 2011). Various studies have described a possible neuronal migration from the PThE to the subpallium (Hetzel 1974, 1975; García-López et al. 2008; Abellán et al. 2010a; Medina and Abellán 2012). These results essentially refer to the subpallial extended amygdala (EA) and septum (Se). The PThE also has been implicated in the mouse as a source of migrating cells that enter the developing pallium (e.g., *Lot1*-, *Gdf10*- and *Tbr2*-expressing neurons; Ruiz-Reig et al. 2017). There is also a subpopulation of Cajal–Retzius neurons invading layer 1 of the developing isocortex which was reported to originate at the PThE (review in Puelles 2011). Other eminential populations may colonize also the accessory olfactory bulb and the NLOT nucleus (Puelles et al. 2000, 2019; Soriano and Del Rio 2005; Remedios et al. 2007; Cabrera-Socorro et al. 2007; García-López et al. 2008; Abellán and Medina 2008, 2009; García-Moreno et al. 2010; Abellán et al. 2010a; Medina and Abellán 2012; Huilgol et al. 2013; Ruiz-Reig et al. 2018).

We were intrigued by the apparent progressive late-developmental diminution and dispersion of the initially dense and massive chicken PThE population, suggestive of either cell death or tangential migration of many PThE-derived neurons. To examine this point, we performed a detailed mapping of *Tbr1* expression in the chicken PThE, examining also neighbouring septal, subpallial, amygdalar, hippocampal and hypothalamic areas at selected medium to late-embryonic stages and in three planes of section. Another point examined with various complementary markers was the relationship of PThE derivatives with the dorsal migratory expansion of the paraventricular area at the telencephalic stalk, correlative with the formation of the medial amygdala homolog (Bardet et al. 2008). Our anatomic reference was the chicken stereotaxic atlas of Puelles et al. (2007, second edition in 2019).

Materials and methods

Animals

All experimental protocols and handling, use, and care of laboratory animals were conducted in compliance with the current normative standards of the European Union (Directive 2010/63/EU), the Spanish Government (Royal Decree 1201/2005 and 53/2013; Law 32/107), and the approval of the University of Murcia committee for animal experimental ethics.

Fertilized chick (*Gallus gallus*) eggs from commercial sources were incubated at 37 °C in a forced-draft incubator with humidified atmosphere at 65% until the desired embryonic stage. Embryos were staged according to Hamburger and Hamilton (1951).

Tissue preparation

Embryos were fixed in 4% paraformaldehyde fixative. Brains of stage HH25 to HH35 embryos were dissected and fixed by immersion in 4% paraformaldehyde (diluted in 0.1 M phosphate-buffered, pH 7.4; PB) at 4 °C for 48 h. Embryos from stage HH36 to HH40 were deeply anesthetized and then perfused transcardially with 0.75% NaCl saline solution, followed by phosphate-buffered 4% paraformaldehyde. Dissected brains postfixed in paraformaldehyde were washed in phosphate-buffered 0.1 M, pH 7.4. Brains were processed by in situ hybridization as free-floating sections after embedding in 4% agarose (low-melting point agarose) diluted in PBS 0.1 M and pH 7.4. Sections 80–90 µm-thick were obtained in horizontal, sagittal or coronal planes using a vibratome, and were processed further as free-floating sections (Ferrán et al. 2015).

In situ hybridization

Brains were processed for in situ hybridization with digoxigenin-UTP-labeled antisense riboprobes. Riboprobes for *Tbr1* (NM 003641638, size 2000 bp, positions 147–2032), *Otp* (NM 011021.2, size 412 bp, positions 179–592) and *Foxg1* (NM 205193., size 633 bp, position 1153–1786) were synthesized from plasmids kindly provided by JL Rubenstein (*Tbr1*), A Simeone (*Otp*) and K Yun (*Foxg1*). The hybridizations on floating vibratome-sections were done according to the standard protocol reported by Ferrán et al. (2015). As general in situ hybridization (ISH) controls, sense and antisense probes were applied to adjacent representative sections

(the signal was present only with antisense probe), and some sections were processed without either sense or antisense probes, to check for possible background due to the other reactives used in the standard ISH procedure. To detect the hybridized product, sections were incubated overnight with alkaline phosphatase-conjugated antidigoxigenin Fab fragments (1:3500, Roche Diagnostics, Manheim, Germany), and nitroblue tetrazolium/bromochloroindolyl phosphate (NBT/BCIP) was used as chromogenic substrate for the final alkaline phosphatase reaction (Boehringer, Mannheim, Germany).

Imaging

Digital microphotographs were obtained with a Zeiss Axiocam camera (Carl Zeiss, Oberkochen, Germany) or with a ScanScope digital slide scanner (Aperio, Vista, CA, USA), and the images were corrected for contrast and brightness using Photoshop CS6 (Adobe Systems, San Jose, CA, USA). All plates were produced and labeled in Adobe Illustrator CS6 software (Adobe Systems, San Jose, CA, USA).

Results

We examined PThE *Tbr1* expression by ISH in coronal, horizontal and sagittal sections of embryonic chick brains at stages HH25-26 (5 days in ovo; 5 d.i.o.), HH29-33 (6.5–7 d.i.o.), HH35 (9 d.i.o.), HH37 (11 d.i.o.), and HH40 (14 d.i.o.). Expression of the *Tbr1* transcription factor is characteristic of glutamatergic neurons in the cerebral cortex and cerebellar nuclei (Englund et al. 2005; Fink et al. 2006); we checked that *Tbr1*-positive cells in the avian PThE are also glutamatergic. Mapping of *Tbr1* in cells emerging from the PThE locus is complicated in practice by similar cells possibly spreading from pallial telencephalic territories nearby (Bulfone et al. 1995; Puelles et al. 2000). It was thus important to identify precisely the original limits of PThE and appropriate anatomic and genoarchitectonic landmarks allowing to assess its subsequent position (Puelles et al. 2000, 2007, 2012; Puelles 2018; Puelles and Rubenstein 2003).

Like any other radial histogenetic unit of the brain wall (Nieuwenhuys and Puelles 2016), the PThE may be conceived as a more or less deformed cuboid in three dimensions, with six faces. The radial dimension connects the ventricular and pial surfaces of the complex through the intervening ventricular and mantle strata. The dorsoventral dimension relates the PThE to the local bordering (dorsal) roof plate structure (basically chorioidal in nature) and to relatively more ventral alar structures also belonging to the prethalamus, namely the central part of the prethalamus (the latter includes the reticular, pregeniculate and subgeniculate nuclei; farther ventrally lies the subcentral complex inclusive of the zona incerta). The terms 'central' and 'subcentral' prethalamus are borrowed with permission from an ongoing companion study on the mammalian prethalamus (Puelles et al. in preparation). Finally, the anteroposterior dimension through the PThE points caudally into the habenular thalamic region (p2), while, rostrally, as explained above, a non-evaginated ventral part of PThE contacts the paraventricular area within the alar peduncular hypothalamus (Pa; PHy; hypothalamic hp1), and a more dorsal evaginated part of both the paraventricular area and the PThE participate in the caudal wall of the interventricular foramen and neighbouring hemisphere, approaching the medial amygdala, pallial amygdala and the hippocampal pallium. Precise boundaries have never been established in this cryptic area.

A constant feature due to its partial evagination is that the avian PThE cuboid is bent upon itself some 90° at the caudal wall of the interventricular foramen (this bend approaches 180° in mammals). As a result, the eminential ventricular surface is convex and relatively expanded (where it participates at both the 3rd and lateral ventricles), while its pial surface oriented into the hemispheric sulcus is concave and significantly compressed upon itself (Fig. 1a, b). The chorioidal roof tela of the prethalamus, which limits dorsally the PThE is similarly bent, extending also partly into the lateral ventricle. An important rostral anatomic landmark at the hypothalamic border of the PThE is the cerebral peduncle, which courses dorsoventrally through the superficial part of the peduncular hypothalamus, passing very close to the whole prethalamo-hypothalamic boundary (Puelles et al. 2012; Puelles and Rubenstein 2015). The peduncle is accordingly useful for topographic delineation of the boundary between Pa (or hypothalamus) and PThE (Figs. 2, 3, 4, 5, 6, 7, 8, 9, 10). Recent molecular studies have suggested that the hypothalamo-telencephalic boundary is marked by the border of expression of the *Foxg1* transcription factor, which may or may not coincide with the border of *Otp* expression in the hypothalamic paraventricular area (Shimogori et al. 2010; Puelles et al. 2012).

Stages HH25/26 (4.5–5 d.i.o.)

Our analysis begins at stages HH25-26, in which eminential neurogenesis is starting. In a caudorostral series of coronal sections taken at the back of the hemisphere (see section plane in Fig. 2j) we already see the *Tbr1*-positive bulge of the PThE at the back of the interventricular foramen, bent upon itself (PThE; ivf; Fig. 2a, b). The eminence displays an incipient strongly *Tbr1*-positive mantle layer and a *Tbr1*-negative ventricular zone, while nearby central areas of the prethalamus are negative (p3; Fig. 2a). The PThE contacts at the back of the hemisphere the primordia of the pallial amygdala and the medial pallium, or prospective hippocampus (PThE; PallA; MPall; Fig. 2a, b). In the next more dorsal sections the PThE is substituted

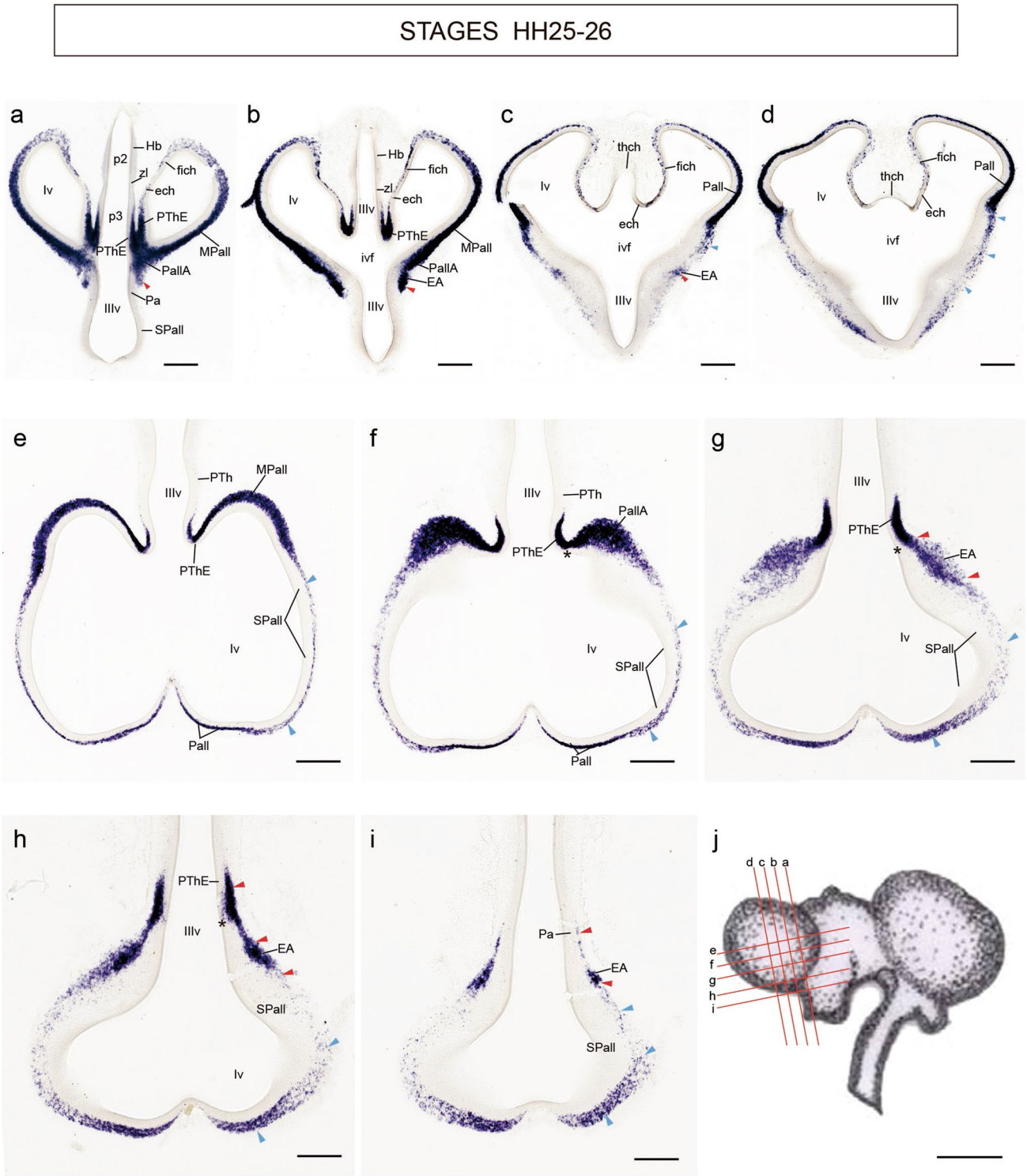

Fig. 2 *Tbr1* expression in the prosencephalon at stage HH25-26. **a–d** Caudorostral series of coronal sections through the caudal part of the telencephalic hemispheres. The bulge of the PThE is visible at the back of each hemisphere, strongly positive for *Tbr1* (**a**, **b**). **e–i** Dorsoventral series of horizontal sections through the rostral prosencephalon. The rostral end of PThE abuts the caudal prospective hippocampus (MPall) (**e**), and the pallial amygdala (PallA). **j** Schema of an HH26 embryonic brain, illustrating the plane of the sections shown in **a–i**. Red arrowheads in **a–c** and **g–i** point to putative migrated neuroblasts moving from the PThE to the Pa and the extended amygdala (EA), while blue arrowheads in **c–i** point to putative pallial neurons migrated subpially into the subpallium. Black asterisks in **f–h** indicate the terminal sulcus. Scale bars in **a–i**, 300 µm, and in **j**, 2.5 mm

by the chorioidal roof area, represented by the thalamic median roof of the 3rd ventricle (thalamic chorioidal tela: thch; Fig. 2c, d), which is continuous bilaterally with lateral portions of chorioidal tissue extending into the medial wall of the hemisphere (anlage of the chorioidal fissure). The proximal bent part of this lateral tela is interpreted here as eminential (prethalamic) chorioidal tela, since it attaches at the underlying PThE (best seen in sagittal sections; Fig. 1a) (ech; Fig. 2a–d, compare PThE in Fig. 2a, b). The distal rest of the lateral roof tissue represents the complementary telencephalic hippocampal tela, which attaches at the fimbrial hem (fich; Fig. 2a, b). Sporadic *Tbr1*-positive cells are seen along the ech and fich chorioidal roof tissue (migrated from subjacent alar plate?), but not in the thch.

Horizontal sections in Fig. 2e–i (see section plane in Fig. 2j) offer a complementary view, illustrating the *Tbr1*-positive PThE primordium as a tongue-shaped distinct portion of the diencephalic neural wall at the back of the interventricular foramen, which clearly bends from the evaginated hemisphere wall into the diencephalon (PThE; Fig. 2e, f). Under the interventricular foramen the rostroventral continuation of the PThE appears as a tapering flat *Tbr1*-positive domain (PThE; Fig. 2g, h), which finally ends short of the paraventricular hypothalamic area (PThE; Pa; Fig. 2i). In this section plane it is easier to assess that the dorsalmost rostral PThE primarily contacts laterally the caudal end of the prospective hippocampus (or medial pallium). This occurs underneath the horizontal section levels where the chorioidal roof would separate them (PThE; MPall; Fig. 2e; compare Fig. 2b). Immediately below this PThE-MPall contact, and nearer to the hemispheric stalk, the eminence also contacts rostrolaterally the pallial amygdala, a thicker *Tbr1*-positive primordium which borders rostrally with the subpallium (PThE; PallA; SPall; Fig. 2f). As observed above in coronal sections (and in Fig. 1a), the PThE also extends *under* the PallA, adopting a flat shape at the bottom of the hemispheric stalk region (PThE: Fig. 2g, h); note that at later stages the entire rostral ventricular surface of the PThE subdomain next to the interventricular foramen will form the diencephalic bank of the future terminal sulcus, establishing the contrast of the eminential *Tbr1*-positive bank with the subpallial *Tbr1*-negative bank of the terminal sulcus in the ventricular relief (asterisk in Fig. 2f–h; compare Fig. 3n–p). The terminal sulcus is a remnant of the caudally evaginated portion of the lateral ventricle at the levels of the amygdalo-hippocampal primordia. However, the underlined useful molecular contrast at its banks should not be confused with the true tel-diencephalic boundary, because this separates one from another the PThE and amygdalo-hippocampal territories, both of them *Tbr1*-positive (the marker *Foxg1* approximates this boundary, leaving the PThE negative; see Fig. 3i, j).

At these subforaminal (extratelencephalic) levels we observe that the rostral border of the PThE is continuous with what appears to be a migratory stream of *Tbr1*-positive cells in the subpial mantle, which reaches the neighbouring hemisphere under the PallA, that is, at the presumptive extended amygdala area (red arrowheads; EA; Fig. 2g–i; see also red arrowheads in Fig. 2a–c). The identification of EA is consistent with observations at subsequent stages and other observations; see "Discussion"). In contrast, the telencephalic subpallium contains only isolated *Tbr1*-positive cells, which apparently migrate out of the neighbouring pallium, and do not reach the EA (blue arrowheads; Fig. 2c–i). In the following we will call the subpial PThE-EA stream the peripeduncular eminential migratory stream for reasons that will be obvious in Fig. 3. More ventrally, where the PThE contacts rostrally the hypothalamus, we see that the incipient *Tbr1*-negative mantle of the hypothalamic paraventricular area is covered by a thin marginal layer of positive cells probably migrated likewise from the PThE (red arrowhead; Pa; Fig. 2i). This hypothalamic migration will later expand deep to the peduncle, and we therefore called it the juxtapeduncular eminential migratory stream. Caudally, the PThE limits beyond the zona limitans (zl) with the unlabelled habenular thalamic domain (Hb; zl; Fig. 2a, b).

Stages HH29-30 (6.5–7 d.i.o.)

At stages HH29-30, the *Tbr1*-expressing PThE mantle is distinctly thicker than at stages HH25-26. Our analysis of this and subsequent stages indicates that it is characteristic of the PThE that its thick *Tbr1*-positive mantle extends uniformly from the ventricle to the pia, irrespective whether it displays a ventricular convex bulge (e.g., PThE in Fig. 3a, b, e, f, n–p), or adopts finally a relatively flat ventricular surface next to the hypothalamus (Fig. 3q). Note the peduncle is now present as a distinct *Tbr1*-negative hypothalamic landmark (pe; Fig. 3a–d, g, p, q).

Coronal, sagittal and horizontal sections (Fig. 3a–l) illustrate that, as before, the PThE essentially remains bent upon itself at the back of the now relatively reduced interventricular foramen, and in dorsal contact with the eminential chorioidal roof specialization (PThE; ech; see also fich; Fig. 3c, d). It also contacts the habenular thalamic area caudally (Hb; Fig. 3a, b). Rostrally the *Tbr1*-positive PThE bends partly into the hemispheric evagination, and is continuous most dorsally with the evaginated hippocampus, their contact occurring just under the chorioidal roof tissue (PThE; Hi; relationship best seen in Fig. 3m, n; see also ech and fich in Fig. 3c, d, e–h). Below the Hi, and below the interventricular foramen, the eminence contacts the pallial amygdala, which at this stage still lies partly rostral to the PThE, projecting

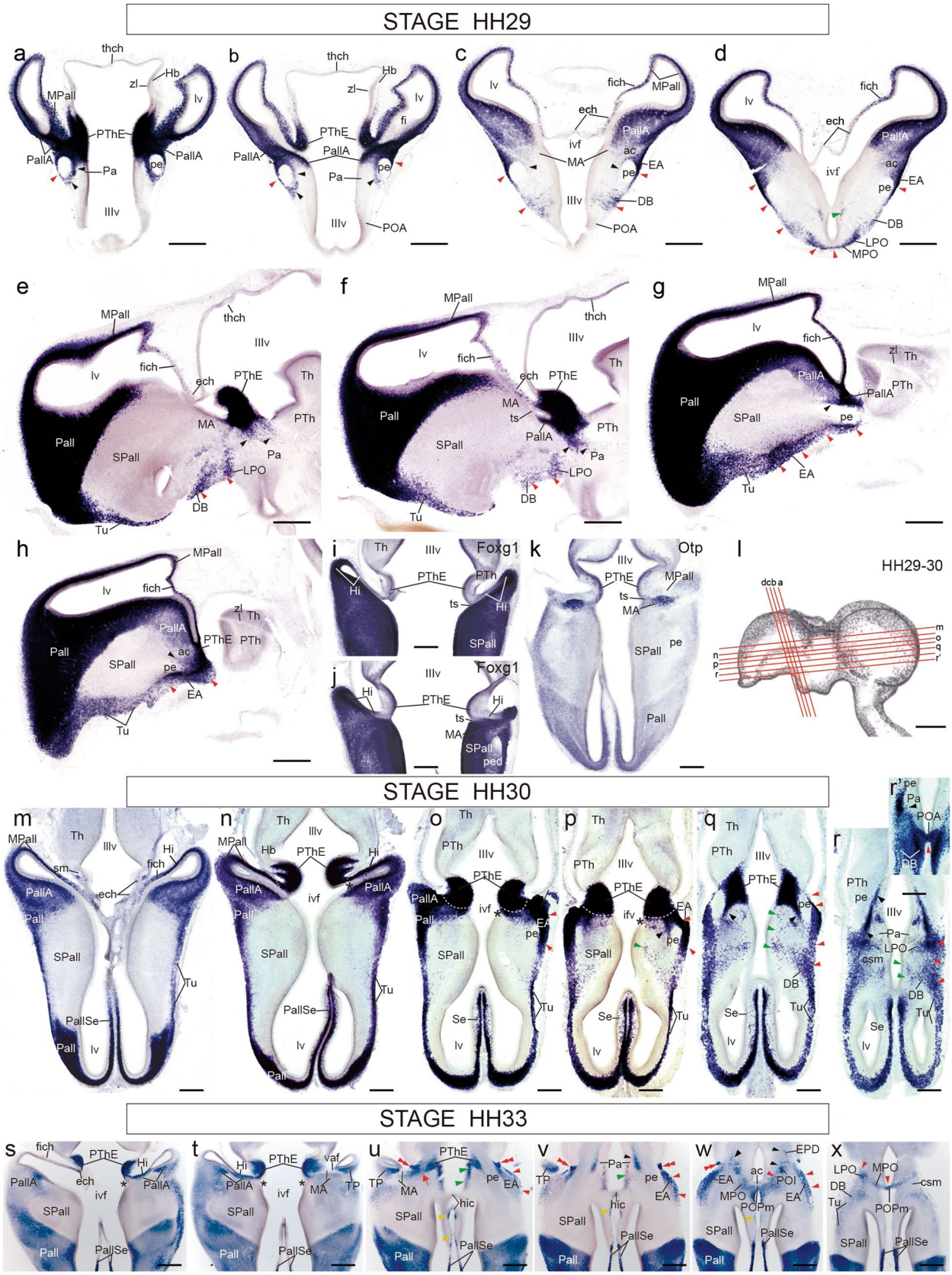
STAGE HH29
a
thch
Hb
zl
lv
MPall
PThE
PallA
Pa
pe
IIIv
b
thch
Hb
zl
lv
fi
PThE
PallA
Pa
pe
IIIv
POA
c
lv
fich
MPall
ech
PallA
ivf
ac
MA
EA
pe
IIIv
DB
POA
d
lv
fich
ech
PallA
ivf
ac
pe
EA
DB
LPO
MPO
e
MPall
thch
IIIv
lv
fich
ech
PThE
Th
PTh
MA
Pall
SPall
Pa
LPO
DB
Tu
f
MPall
thch
IIIv
lv
fich
Th
ech
PThE
MA
ts
PallA
PTh
Pall
SPall
Pa
LPO
DB
Tu
g
MPall
lv
fich
zl
Th
PallA
PallA
PTh
Pall
SPall
pe
EA
Tu
h
MPall
lv
fich
zl
Th
PallA
PThE
PTh
Pall
SPall
ac
pe
EA
Tu
i
Th
IIIv
Foxg1
PThE
PTh
Hi
ts
Hi
SPall
j
IIIv
Foxg1
Hi
PThE
Hi
ts
MA
SPall
ped
k
IIIv
Otp
PThE
MPall
ts
MA
SPall
pe
Pall
l
HH29-30
dcb a
m
o
q
r
n
p
r
STAGE HH30
m
MPall
Th
IIIv
Hi
fich
sm
PallA
ech
Pall
SPall
Tu
PallSe
Pall
lv
n
Th
MPall
Hb
IIIv
PThE
Hi
PallA
PallA
ivf
Pall
SPall
Tu
PallSe
lv
Pall
o
Th
PTh
IIIv
PThE
PallA
ivf
Pall
EA
pe
SPall
Se
Tu
lv
p
Th
PTh
IIIv
PThE
EA
ifv
pe
SPall
Se
Tu
lv
q
Th
PTh
IIIv
PThE
pe
DB
Tu
Se
lv
r'
pe
Pa
POA
DB
r
PTh
pe
IIIv
Pa
LPO
csm
DB
Tu
Se
lv
STAGE HH33
s
fich
PThE
Hi
PallA
ech
ivf
PallA
SPall
Pall
PallSe
t
Hi
PThE
vaf
PallA
ivf
MA
TP
SPall
Pall
PallSe
u
PThE
TP
MA
pe
EA
hic
SPall
Pall
PallSe
v
Pa
TP
pe
EA
hic
SPall
Pall
PallSe
w
EPD
EA
ac
POI
MPO
POPm
EA
SPall
Pall
PallSe
x
LPO
MPO
csm
DB
Tu
POPm
SPall
PallSe

◂**Fig. 3** Expression of *Tbr1*, *Foxg1* and *Otp* in the prosencephalon at stages HH29-33. **a–d** Caudorostral series of coronal sections through the caudal part of the telencephalic hemispheres at HH29, showing *Tbr1* expression. **e–h** Mediolateral series of parasagittal sections through the rostral prosencephalon at HH29, showing *Tbr1* expression. **i–j** Horizontal sections through the rostral prosencephalon at HH30, showing *Foxg1* expression. This gene is expressed selectively in the telencephalon (in mouse, except for the dentate gyrus primordium); the PThE is negative for this marker. **k** Horizontal section through the medial amygdala (MA) at HH30, showing *Otp* expression (implying neurons migrated tangentially from the paraventricular hypothalamic area). **l** Schema of an HH30 embryonic brain a, illustrating the plane of the sections shown in **a–d** and **m–r′**. **m–r′** Dorsoventral series of horizontal sections through the rostral prosencephalon at stage HH30, reacted for *Tbr1*; the green arrowheads (**p–r**) mark the apparent initial stage of the periventricular eminentio-septal migration stream. **s–x** Dorsoventral standard horizontal vibratome series through the rostral prosencephalon at stage HH33 labelled with *Tbr1*. The periventricular eminentio-septal migratory stream is now clearly observable (green arrowheads in **u**, **v**). Red arrowheads in **a–h**, **o–r′** and **u–x** point to the peripeduncular migratory stream. Double red arrowheads in **u–w** point to the hypothalamic component of the peripeduncular migratory stream. Black arrowheads in **a–h**, **p–r′** and **v–w** point to the juxtapeduncular migratory stream. Yellow arrowheads in **u–w** point to the septo-commissural migratory stream. Black asterisks in **n–p** and **s–t** indicate the position of the terminal sulcus. Scale bars in **a–k** and **m–x**, 500 µm, and in **l**, 2.5 mm

its ventricular zone into the rostral bank of the terminal sulcus (PallA; Fig. 3a, b, g, h, n, o). A terminal sulcus is now well visible, but is unlike the definitive one in having *Tbr1*-positive domains (eminential and pallial amygdalar) at its two banks (PThE; PallA; Fig. 3a, b; see ts in Fig. 3f, i–k; asterisk in Fig. 3o, p). Note in Fig. 3m–o the relationship of the terminal sulcus with the overlying caudal recess of the lateral ventricle and the amygdalo-hippocampal pallial region, as compared with the moderately bulging *Tbr1*-negative subpallial region. The position in horizontal sections of the tel-diencephalic boundary at the PThE/PallA-Hi interface was traced with white dashes (Fig. 3n–p), partly on the basis of differential expression of *Foxg1* in the telencephalon (Fig. 3i, j; Hatini et al. 1994). Note also the neighbouring medial amygdala (MA; Fig. 3k), which we identified next to the terminal sulcus with the *Otp* marker, according to Bardet et al. (2008; see "Discussion"). Finally, the eminential border with the *Tbr1*-negative hypothalamic paraventricular area is maintained (PThE; Pa; Fig. 3a, b, e, f, r, r′); it shows groups of *Tbr1*-positive eminential cells passing into the paraventricular area (the juxtapeduncular stream; black arrowheads; Pa; Fig. 3e, f; see also Morales-Delgado et al. 2011, 2014).

Indeed, both the peripeduncular and juxtapeduncular eminential migration streams we described at the earlier stage are now better developed and more massive. The peripeduncular stream clearly sorts superficially out of the PThE under the pallial amygdala, and then surrounds the peduncle along the hemispheric stalk, first dorsally and then laterally, always subpially (red arrowheads in Fig. 3a–h, p–r). The majority of its cells seem to reach the extended amygdala (red arrowheads; EA, Fig. 3b–d, g, h, o, p). Other superficial cells of the peripeduncular stream seem to diverge medialward into the preoptic area, which they cross from lateral to medial, approaching the median preoptic region that subsequently forms superficial to the crossing of the anterior commissure (red arrowheads; LPO; MPO; Fig. 3d–f, r, r′). Others bypass the EA and the preoptic area and enter the diagonal band domain of the subpallium, advancing therein towards the septum (red arrowheads; DB; Fig. 3c–f, q, r). The diagonal band cells lie close to the gradiental tapering end of the migration of pallial *Tbr1*-positive cells that invades the surface of the olfactory tuberculum (Tu; Fig. 3e–h, m–r).

The juxtapeduncular stream sorts out of the PThE at intermediate mantle levels and penetrates the rostrally lying hypothalamic paraventricular area just superficial to the negative paraventricular nucleus, and deep to the peduncle (prospective lateral hypothalamus; black arrowheads; Fig. 3a–c, e–h, p–r, r′). The derivatives seem to be the local sector of the lateral hypothalamus and the dorsal entopeduncular nucleus (see below). This stream may also contribute some cells to the preoptic area and the diagonal band, due to the fact that the peripeduncular and juxtapeduncular streams fuse together at the rostral border of the peduncle (Fig. 3a, b, left side).

At this stage we saw also evidence of a third eminential migration, represented by a periventricular pathway identified by us as an eminentio-septal migratory stream. This deep stream courses rostralward under the interventricular foramen until it reaches the roof plate area of the preoptic area, occupied by the anterior commissure, and enters the septal commissural plate caudally to that commissure. This stream is rather discontinuous at stage HH30, when we first observed it (green arrowheads; Fig. 3d, p–r), but is much better developed, though still a bit discontinuous, at stage HH33 (green arrowheads; Fig. 3u, v).

Stages HH33-HH34 (8 d.i.o)

A horizontal HH33 series and coronal and sagittal HH34 series of sections illustrate two singular morphogenetic changes in the telencephalon, which are of interest for the present analysis. On one hand, there is a marked increase in the size of the pallium as a whole. The amygdalo-hippocampal pallial pole results pushed outwards and backwards, and forms a diminutive 'temporal pole' (TP; Figs. 3t–v, 4a–c). This process stretches at the back of the hemisphere the fimbrial chorioidal tela, as well as the thin hippocampal cortical primordium found under it (fich; Hi; Figs. 3s, t, 4a–d), tending to separate the latter from its earlier contact with the evaginated part of the PThE (PThE; Hi; Figs. 3s–u, 4c). Underneath the remnant of this contact we see a caudal surface of the hemisphere that is *Tbr1*-negative; we think

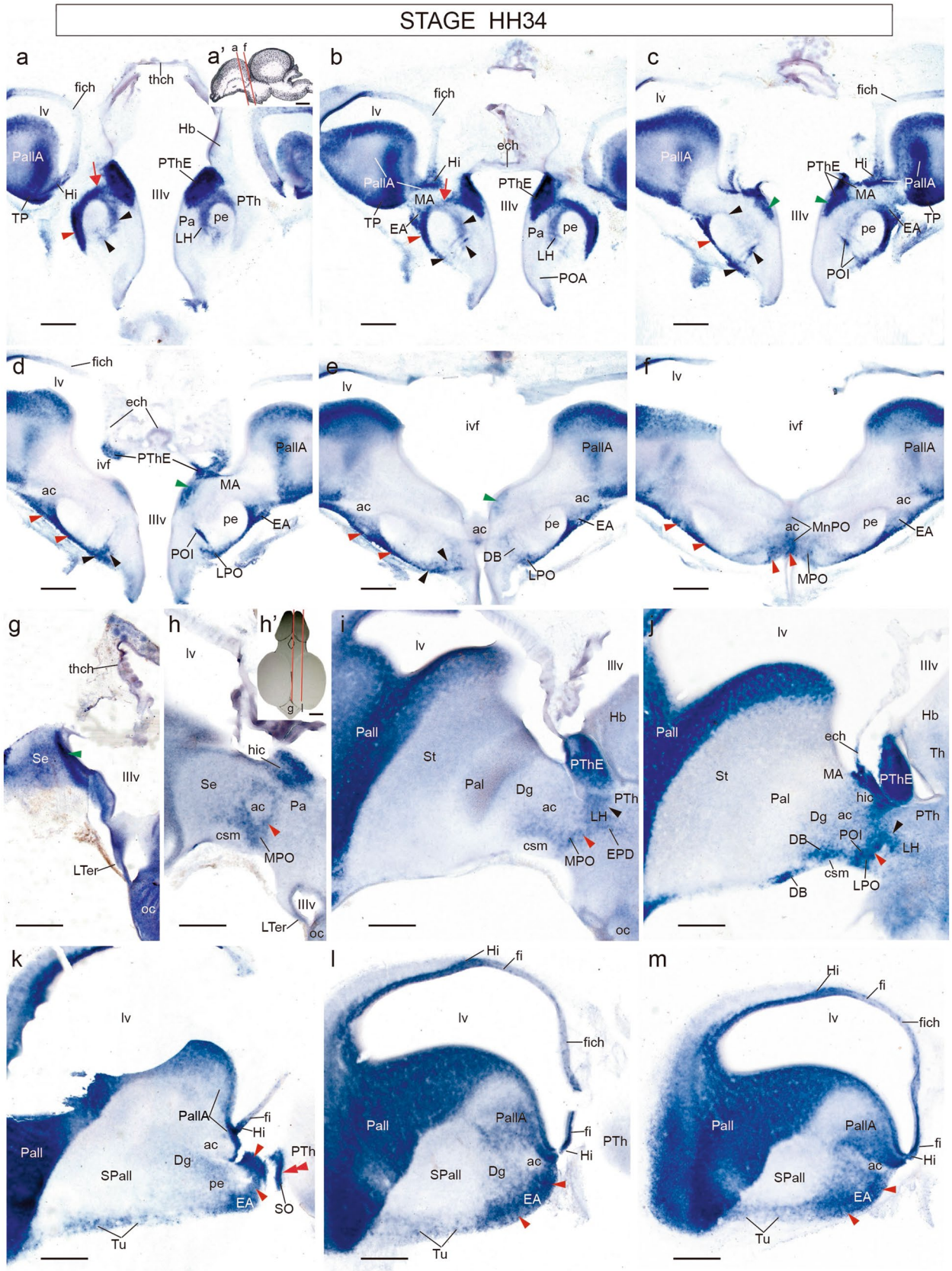
STAGE HH34
a
a'
a f
fich
thch
lv
Hb
PallA
PThE
Hi
IIIv
PTh
TP
Pa
pe
LH
b
ech
MA
EA
POA
c
POI
d
ivf
ac
LPO
e
DB
f
MnPO
MPO
g
Se
LTer
oc
h
h'
hic
csm
i
Pall
St
Pal
Dg
EPD
j
Th
k
SPall
Tu
SO
l
m

◂**Fig. 4** *Tbr1* expression in the prosencephalon at stage HH34. **a–f** Caudorostral series of coronal sections through the caudal part of the telencephalic hemispheres. **a′** Schema of an HH34-36 embryonic brain, illustrating the planes of the sections shown in **a–f**. **g–m** Mediolateral series of parasagittal sections through the rostral prosencephalon. The inset **h′** is a drawing indicating the mediolateral range of the sagittal sections shown. Red arrowheads in **a–f** and **h–m** point to the telencephalic component of the peripeduncular migratory stream. Red double arrowhead in **k** points to the hypothalamic component of the peripeduncular migratory stream. Black arrowheads in **a–e** and **i–j** point to the juxtapeduncular migratory stream. Green arrowheads in **c–e** point to the eminentio-septal migratory stream. Red arrows in **a**, **b** point to the bridge of cells connecting the PThE with the peripeduncular migratory stream. Scale bars in **a–m**, 500 µm, and in **a′** and **h′**, 2.5 mm

this possibly corresponds to the pial surface of the medial amygdala, which lies close to the neighbouring temporal pole (MA; TP; right side in Fig. 3t; left side in Figs. 3u). At the same time, the pallial amygdala is also pushed laterally; as a consequence, its earlier subforaminal extension results stretched into a very thin corridor passing over the medial amygdala; this amygdalar pallial corridor apparently still retains contact with the PThE at some points (PallA; PThE; MA; Figs. 3s, t, 4b, c). The reduction of the presence of the pallial amygdala territory at the terminal sulcus, particularly medially, causes a part of the subpallium (probably the diagonal area; see Fig. 4i) to become the partner of the PThE at the banks of that sulcus (asterisks; Fig. 3s, t). That is, the early PThE-pallial terminal sulcus is substituted by a PThE-subpallial sulcus. Sagittal HH34 material in Fig. 4g–l demonstrates that in medial sections the PThE secondarily limits (or seems to limit) with the subpallium across the terminal sulcus (Fig. 4h, i), whereas more laterally there is a transition into PThE limiting with the stretched corridor of the pallial amygdala (Fig. 4j, k).

On the other hand, we also observe a marked increase in the size of the *Tbr1*-negative subpallial septum, compared to its scarce extension at stages HH29/30 (compare Fig. 3q, r with Figs. 3s–x, 4g). It seems improbable that this can be due to a local septal proliferative increment. We think rather that it may be an indirect effect of global hemispheric morphogenesis, by which redistribution of increasing pallial masses around the subpallium as a whole generates forces that may push medial portions of subpallium which initially developed at the external or ventral hemispheric wall into the medial (septal) wall. We conclude that in the chick these septal changes occur between stages HH30 and HH33. Current models of subpallial subdivision emphasize the adult extension of striatal, pallidal and diagonal subpallial molecular sectors into the septal wall (Puelles et al. 2013, 2016a).

This morphogenetic enlargement of the subpallial septum coincides with bilateral appearance of a thin marginal line of *Tbr1*-positive cells which apparently sort out of the strongly *Tbr1*-positive pallial septum, and advance through the negative subpallial septum into the area of the incipient hippocampal commissure (PallSe; yellow arrowheads; hic; Fig. 3t–w). We call this transient septal formation the septo-commissural migratory stream. The telencephalic commissural plate lies at the midline of the subpallial septum, forming the rostralmost component of the forebrain roof plate.

As regards the eminential migration streams at HH33, we note first that the peripeduncular stream is still partly connected with the PThE, though the bridge of connecting cells is no longer massive (red arrow; Fig. 3u; left side; Fig. 4a, b). Moreover, as the peripeduncular eminential cells pass around the peduncle, they divide now into two neighbouring, but separate streams. One of them seems less compact now, and clearly continues subpially beyond the peduncle into the telencephalic extended amygdala (red arrowheads; EA; Figs. 3u–w, 4a–f, k–m). Some of its cells reach as well the lateral preoptic area and the diagonal band (red arrowheads; LPO; DB; Figs. 3x, 4d,e,i). Out of LPO a good number of positive cells extend linearly medialwards (along the preoptic marginal stratum), passing through the medial preoptic area into the median preoptic area. Many positive cells accumulate there, particularly superficially to the incipient anterior commissure (red arrowheads; MPO, MnPO; Figs. 3w, x, 4d–f, h; compare Fig. 3d–f). The other peripeduncular stream is smaller, but very compact, and courses around the peduncle strictly outside the telencephalon, apparently within the paraventricular hypothalamic area (double red arrowheads; Figs. 3u–w, 4k). This smaller but dense subpial mass will finally stabilize in the area of the supraoptic nucleus (SO; Fig. 4k).

The juxtapeduncular stream which coursed deep to the peduncle builds by this stage a tapering *Tbr1*-positive cell population within the lateral hypothalamus (LH) adjacent to the negative paraventricular nucleus (black arrowhead; LH; Pa; Figs. 3v, 4a, b, i, j). Other derivatives of this stream apparently include a small dorsal entopeduncular cell group (EPD), as well as what we call the '*preoptic island*' (POI), a rounded positive cell aggregate found at the dorsal end of the positive HL area (black arrowheads; EPD; POI; Figs. 3w, 4i, j).

As mentioned above, the eminentio-septal stream is first clearly distinct at HH33. It sorts out of the PThE at the same horizontal level as the other streams, but selectively courses rostralward through the periventricular stratum, and approaches the septal commissural plate passing under the interventricular foramen (green arrowheads; Fig. 3u, v). Its cells apparently do not yet reach the median septal territory at this stage, where they are preceded by some of the *Tbr1*-positive pallial septal migrated elements. In contrast, some *Tbr1*-positive cells of the eminentio-septal stream penetrate the septal commissural plate at HH34, moving past the anterior commissure into the area of the hippocampal commissure (ac; hic; Fig. 4h).

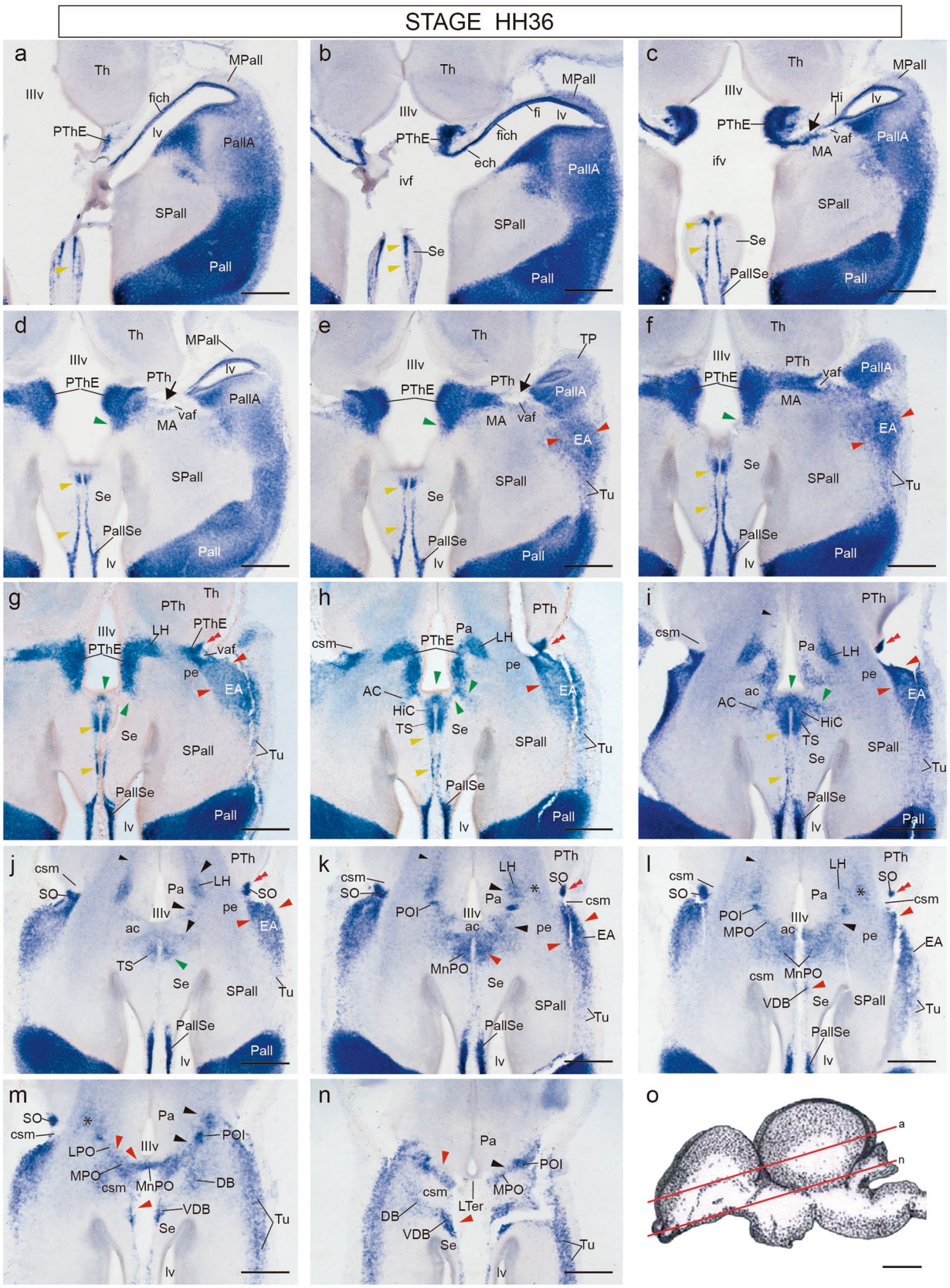
STAGE HH36
a
Th
MPall
IIIv
fich
PThE
lv
PallA
SPall
Pall
b
Th
MPall
IIIv
fi
lv
PThE
fich
ech
PallA
ivf
SPall
Se
Pall
c
Th
MPall
IIIv
Hi
lv
PThE
vaf
PallA
MA
ifv
SPall
Se
PallSe
Pall
d
Th
MPall
IIIv
lv
PThE
PTh
PallA
vaf
MA
SPall
Se
PallSe
lv
Pall
e
Th
TP
IIIv
PTh
PThE
PallA
MA
vaf
EA
SPall
Tu
Se
PallSe
lv
Pall
f
Th
IIIv
PTh
PThE
vaf
PallA
MA
EA
Se
SPall
Tu
PallSe
lv
Pall
g
Th
PTh
IIIv
LH
PThE
PThE
vaf
pe
EA
Se
SPall
Tu
PallSe
lv
Pall
h
PTh
csm
Pa
PThE
LH
pe
EA
AC
HiC
TS
Se
SPall
Tu
PallSe
lv
Pall
i
PTh
csm
Pa
LH
pe
EA
ac
AC
HiC
TS
SPall
Se
Tu
PallSe
lv
Pall
j
csm
PTh
SO
Pa
LH
SO
IIIv
pe
EA
ac
TS
Se
SPall
Tu
PallSe
lv
Pall
k
csm
PTh
LH
SO
SO
Pa
*
POI
IIIv
csm
ac
pe
EA
MnPO
Se
SPall
Tu
PallSe
lv
l
csm
LH
PTh
SO
SO
Pa
*
csm
POI
IIIv
MPO
ac
pe
EA
csm
MnPO
VDB
Se
SPall
Tu
PallSe
lv
m
SO
Pa
csm
*
POI
LPO
IIIv
MPO
csm
MnPO
DB
VDB
Tu
Se
lv
n
Pa
POI
csm
MPO
LTer
DB
VDB
Se
Tu
lv
o
a
n

◂**Fig. 5** *Tbr1* expression in the prosencephalon at stage HH36. **a–n** Dorsoventral series of horizontal sections through the rostral prosencephalon. **o** Schema of an HH34-36 embryonic brain, illustrating the plane of the sections shown in **a–n**. Black arrows in **c–e** indicate remnants of the earlier connection between the PThE and the amygdalar pallium. Red arrowheads in **c–n** point to the telencephalic component of the peripeduncular migration. Red double arrowheads in **g–l** point to the hypothalamic component of the peripeduncular migration. Black arrowheads in **j–n** point to the juxtapeduncular migration. Small black arrowheads in **i–l** point to a small hypothalamic component of the periventricular migration. Yellow arrowheads in **a–i** point to the septo-commissural migration. Green arrowheads in **d–j** point to the eminentio-septal migration. Black asterisk in **k–m** indicate the position of the dorsal entopeduncular nucleus (EPD). Scale bars in **a–n**, 500 µm, and in **o**, 2.5 mm

Stage HH36 (10 d.i.o.)

A horizontally sectioned series at HH36 shows a very similar pattern in most aspects, but shows more advanced development of the eminentio-septal migration. Dorsal sections display the stable relationships of the partially evaginated PThE with the eminential chorioidal tela, in lateral continuity with the fimbrial tela (ech, fich Fig. 5a, b). The third section shown is alevel with the terminal sulcus and contains the lateral continuity of PThE with pallial amygdala (under the sulcus) and also with the neighbouring caudal tip of the hippocampus (PThE; PallA; Hi; Fig. 5c). The neighbourhood of the medial amygdala also shows some dispersed positive cells (MA; Fig. 5c–f). The eminentio-amygdalar *Tbr1*-positive bridge is partly disrupted by the passage of a thin rounded fibre tract, which we think is the ventral amygdalofugal tract (vaf; Fig. 5c–e; check Puelles et al. 2007, 2019; particularly Atlas Figures 94–95). This tract also can be seen more ventrally, traversing subpially the peripeduncular migratory stream (vaf; Fig. 5f, g), before it incorporates into the peduncle. At these various levels the PThE continues showing a compact *Tbr1*-positive population throughout its thickness. It bulges medially into the 3rd ventricle (PThE; Fig. 5c–i), but hardly rostrally, into the reduced interventricular foramen (PThE; Fig. 5b, c).

The eminentio-septal migratory stream is now better developed. It is formed by a voluminous periventricular *Tbr1*-positive population that exits the rostral boundary of the PThE, and then proceeds rostralward, always periventricularly, until it reaches the characteristic U-shaped nucleus of the hippocampal commissure (Puelles et al. 2007, Puelles 2018), as well as some other cell groups in the septocommissural region (green arrowheads; Fig. 5d–h). At levels where this stream passes behind the anterior commissure to reach more caudal parts of the septum, some cells diverge, forming bilaterally the nucleus of the anterior commissure (ac; AC; Fig. 5i). The HiC nucleus also receives a separate *Tbr1*-positive migratory stream emanating from the *Tbr1*-positive pallial septum (yellow arrowheads; PallSe; Fig. 5a–i). The HiC population as a whole seems continuous with the large mass of the similarly labelled triangular septal nucleus, which ends just at the level of the anterior commissure (HiC; TS; ac; Fig. 5h–j). The TS is substituted under the commissure by the median preoptic cell group (MnPO) apparently migrated separately via the peripeduncular stream and the LPO and MPO areas (red arrowheads; Fig. 5j, k), though some of these cells might as well come via the juxtapeduncular stream and the POI (black arrowheads; Fig. 5l–n).

The juxtapeduncular migratory stream appears at this stage somewhat discontinuous, possibly indicating that the migration per se has ended, and resulting eminentia-derived formations are becoming stabilized and differentiated at various positions. The major derivative of this intermediate stream is the lateral hypothalamic area adjacent to the unlabelled paraventricular nucleus; the LH occupies the intermediate stratum of the Pa area, deep to the peduncle (LH; Pa; pe; Fig. 5g–l). This population shows in the more ventral sections a tapering trail of labelled cells that extend into the underlying hypothalamus, following the peduncle (small black arrowheads: Fig. 5i–l). Rostral to LH there appear 2–3 islets of positive cells, which converge rostromedially into the *medial preoptic area* (MPO; Fig. 5l–n). There is a salient preoptic island in this area which repeatedly shows a particularly dense *Tbr1*-positive cell population. This seems not to have been described previously; we named it tentatively the preoptic island (POI; Fig. 5k–n).

The peripeduncular migratory stream is still clearly visible, and remains connected proximally to its eminential apparent source, while it reaches subpially the extended amygdala on the other end (red arrowheads; PThE; ped; EA; Fig. 5e–l). However, as mentioned above, some of these peripeduncular elements diverge from the EA medialwards, entering the neighbouring diagonal band formation. The latter can be followed rostrally into the medial septum, where a relatively compact vertical nucleus of the diagonal band is always observed subpially in our material (DB; VDB; Fig. 5l–n). We also observed again at the hemispheric stalk the separate compact group of peripeduncular migrating elements which remain outside the telencephalic subpallium (double red arrowheads; Fig. 5g–i). We think that this subpial group contributes to the supraoptic nucleus complex (double red arrowheads; SO; Fig. 5j–m).

Stage HH37 (11 d.i.o.)

At HH37, expression of *Tbr1* has diminished in density at the PThE compared with earlier stages (PThE; Figs. 6a–c, 7a–g). *Tbr1*-positive neurons are now most abundant periventricularly, though the earlier characteristic ventricular bulge has diminished (PThE; Figs. 6a–c, 7a–d). The PThE also seems now more distant from the hippocampus and the pallial amygdala, since the stretched pallial corridor connecting

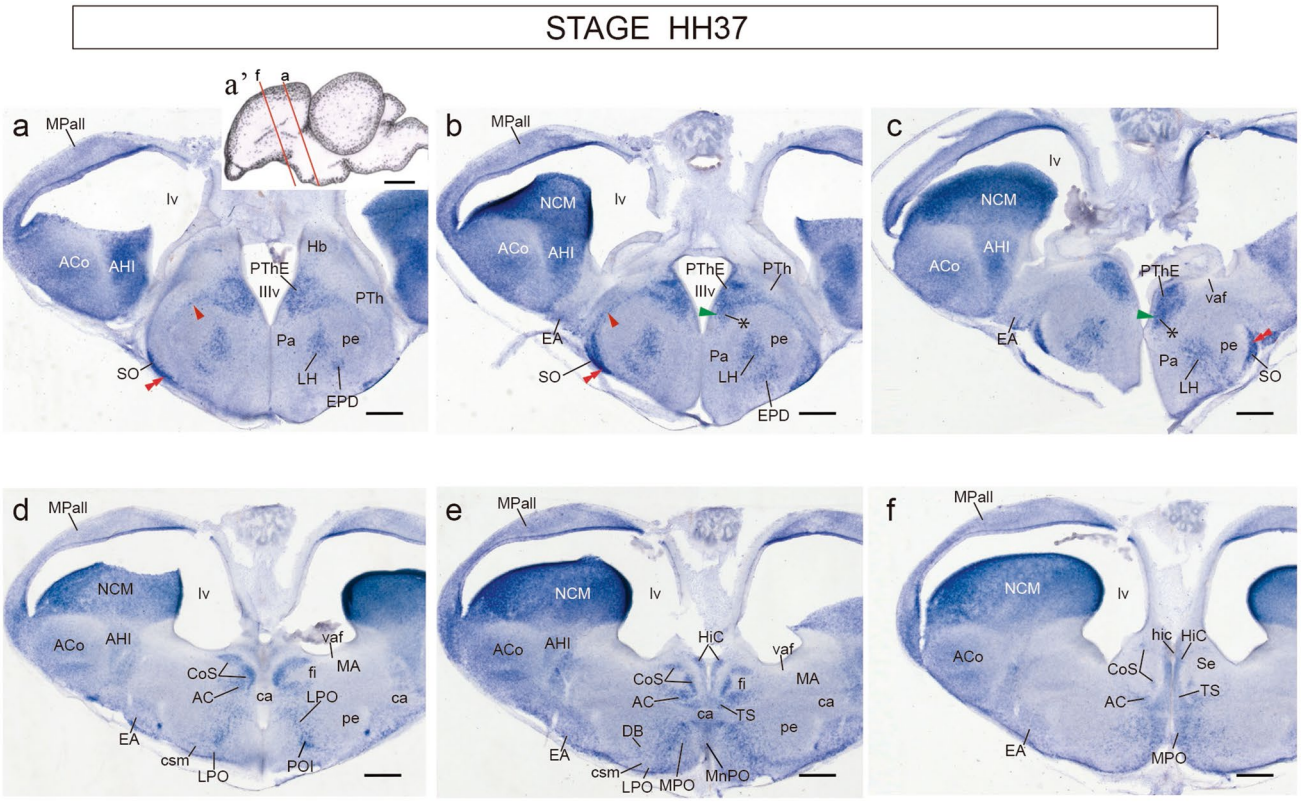

Fig. 6 *Tbr1* expression in the prosencephalon at stage HH37. **a–c** Caudorostral series of coronal sections through the transition from the peduncular hypothalamus and PThE to the telencephalon. **a′** Schema of an HH37 embryonic brain, illustrating the plane of the sections shown in **a–c**. Red arrowheads in **a**, **b** point to the telencephalic component of the peripeduncular migration. Red double arrowheads in **a–c** point to the hypothalamic component of the peripeduncular migration. Black arrowheads in **a**, **b** point to the juxtapeduncular migration. Green arrowheads point to the eminentio-septal migration. Asterisks in **b**, **c** indicate the eminentio-septal cellular bridge. Scale bars in **a–f**, 500 µm, and in **a′**, 5 mm

them previously has largely disappeared. In part this disconnection may be due to the growth of the vaf tract and other accompanying fibre packets exiting the amygdala (vaf; Fig. 7a–c). The PThE thus relates mainly at this stage with several subpallial telencephalic territories, either septal, paraseptal or central -pallidal or diagonal- in nature (Fig. 7a–h; see subpallium model in Puelles et al. 2013, 2016a, b). The *Tbr1*-negative subpallial septal area also has advanced significantly in its massive development (Fig. 7a–m). The former septo-commissural migration stream is no longer visible, and we see only some isolated *Tbr1*-positive septal patches next to the pallio-subpallial boundary, which we tentatively interpreted as the septo-fimbrial nucleus, supposedly a remnant of the septo-commissural migration stream (SFi; Fig. 7a–j).

As regards the eminentio-septal stream, its labelled derivatives within the formerly *Tbr1*-negative septo-commissural area are now strongly developed. We still observed at this stage dense positive cells interconnecting the PThE remnant with the septal CoS and HiC nuclei, suggesting a final phase of this migration; this cellular bridge typically passes under the interventricular foramen (asterisk and green arrowheads; CoS, HiC; Figs. 6b, c, 7a–g). Other septal labelled cells are found at the nucleus of the anterior commissure (AC; Figs. 6d–f, 7g–j) and the triangular septal nucleus (TS; Figs. 6e–i, 7e–h).

The earlier lateral continuity of the PThE with the peripeduncular migration stream appears significantly diminished in cell number now; only a remnant of that transient structure was detected, still stretched over the peduncle (red arrowheads; Figs. 6a, b, 7k, l). This subpial stream leads into extratelencephalic and intratelencephalic derivatives. The intratelencephalic ones connect with a disperse labelled population within the subpallial *extended amygdala* (EA; Fig. 6b–f; also red arrowheads in Fig. 7g–m), while other subpial elements apparently transported by this stream appear more ventrally in association with the diagonal band area (Dg; Fig. 7j–l). Usually we observed a small very dense subpial labelled patch at the medial septal surface, found just rostrally to the csm tract, which we think may correspond to the ventral diagonal band nucleus (VDB; Fig. 7k, l); a possible more disperse horizontal diagonal band counterpart

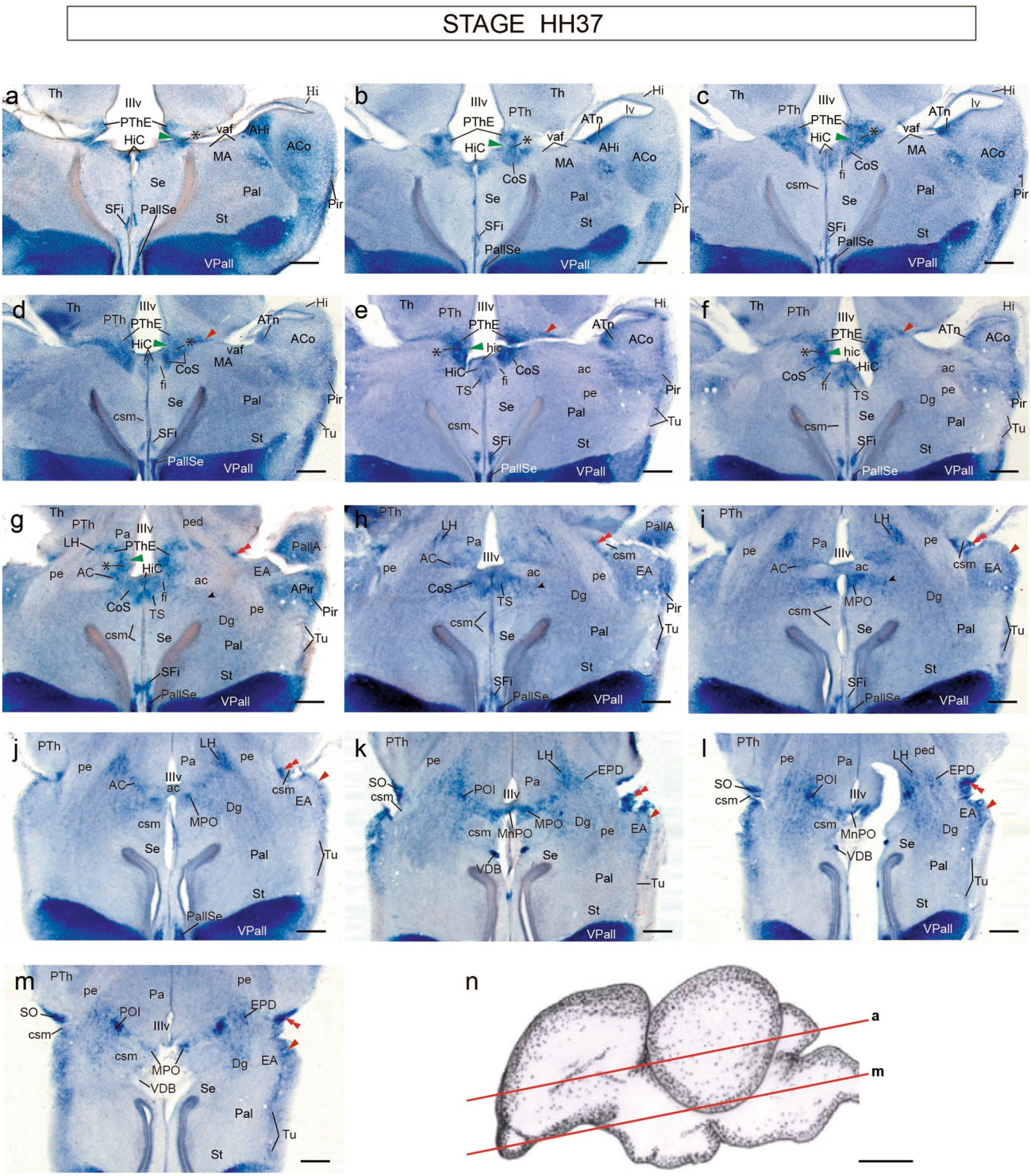

Fig. 7 *Tbr1* expression in the prosencephalon at stage HH37. **a–m** Dorsoventral series of horizontal sections through the rostral prosencephalon at HH37. **n** Schema of an HH37 embryonic brain, illustrating the plane of the sections shown in **a–m**. Red arrowheads in **d–f** and **i–m** point to the telencephalic component of the peripeduncular migration. Red double arrowheads in **g–m** point to the hypothalamic component of the peripeduncular migration. Small black arrowheads in **g–i** point to juxtapeduncular migrated cells dispersed in the diagonal area (Dg). Green arrowheads in **a–g** point to the eminentio-septal migration. Asterisks in **a–g** indicate the eminentio-septal cellular bridge. Scale bars in **a–m**, 500 µm, and in **o**, 5 mm

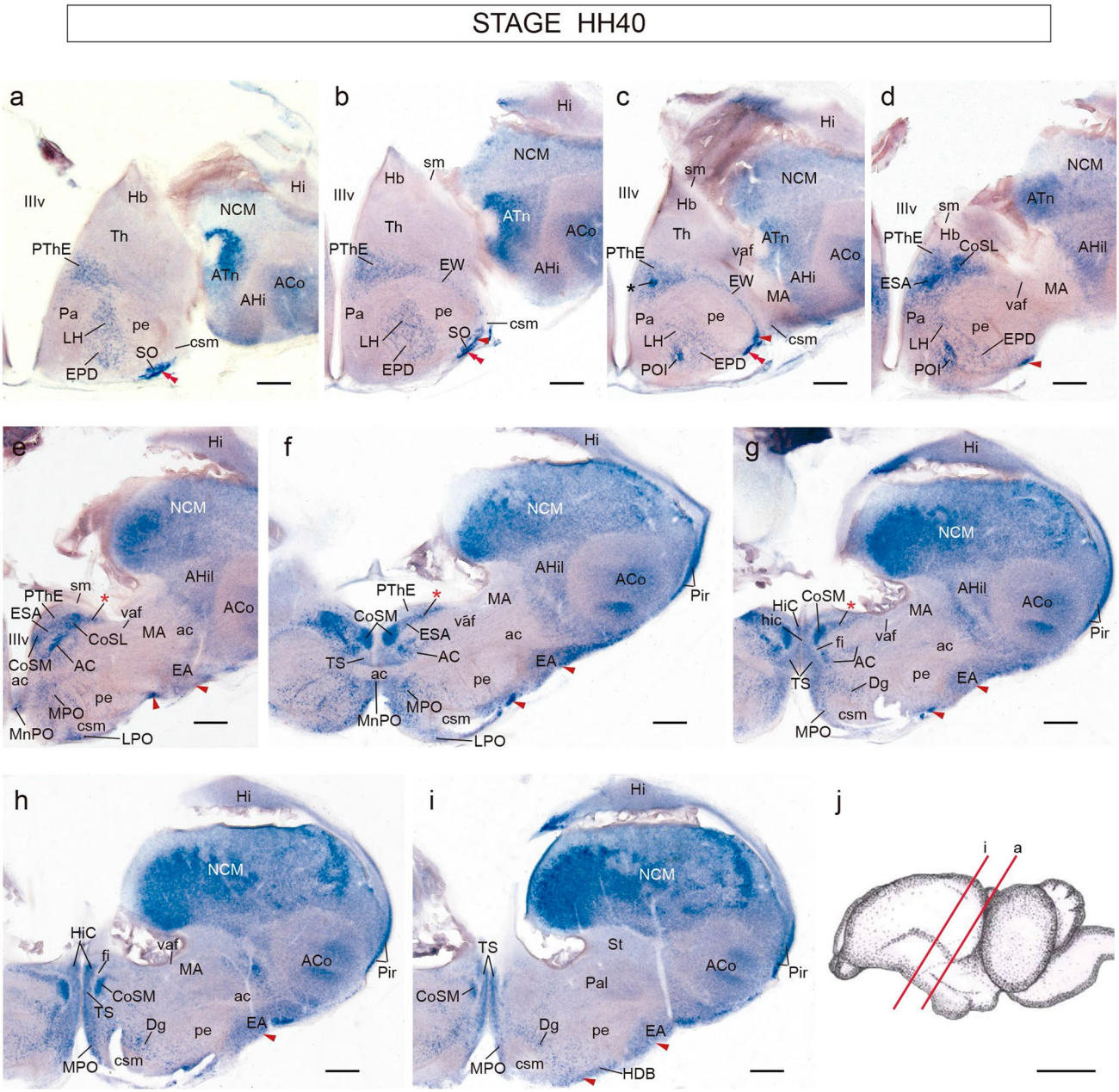

Fig. 8 *Tbr1* expression in the prosencephalon at stage HH40. **a–i** Caudorostral series of oblique coronal sections through the di-telencephalic transition. **j** Schema of an HH40 embryonic brain at HH40, illustrating the plane of the sections shown in **a–i**. Red arrowheads in **b–i** point to the telencephalic remnants of the peripeduncular migratory stream. Red double arrowheads in **a–c** point to the hypothalamic component peripeduncular migration derivatives. Black asterisk in **c** indicates the caudal tip of the eminentio-septal area (ESA). Red asterisks in **e–g** indicate the CoS wing subnucleus. Scale bars in **a–i**, 500 µm, and in **j**, 5 mm

is also visible (HDB; Dg; Fig. 7k–m). In contrast, the subpial extratelencephalic peripeduncular migrated population reported above, which is associated topographically to the hypothalamic paraventricular area, appears at HH37 as a dense and strongly *Tbr1*-positive subpial cell group (e.g., double red arrowheads; Fig. 7g–j) which ends ventrally at the supraoptic nucleus or its immediate neighbourhood (SO; Figs. 6a–c, 7k–m).

The juxtapeduncular stream (found deep to the peduncle) has decomposed, as we already saw one stage before, into distinct populations, which are now more distinctly distinguished. Closest to the PThE, within the peduncular hypothalamus, there is the previously described lateral hypothalamic area (LH), its labelling being restricted to the sector lying external to the negative paraventricular hypothalamic nucleus (LH; Pa; Fig. 7h–m). The LH appears

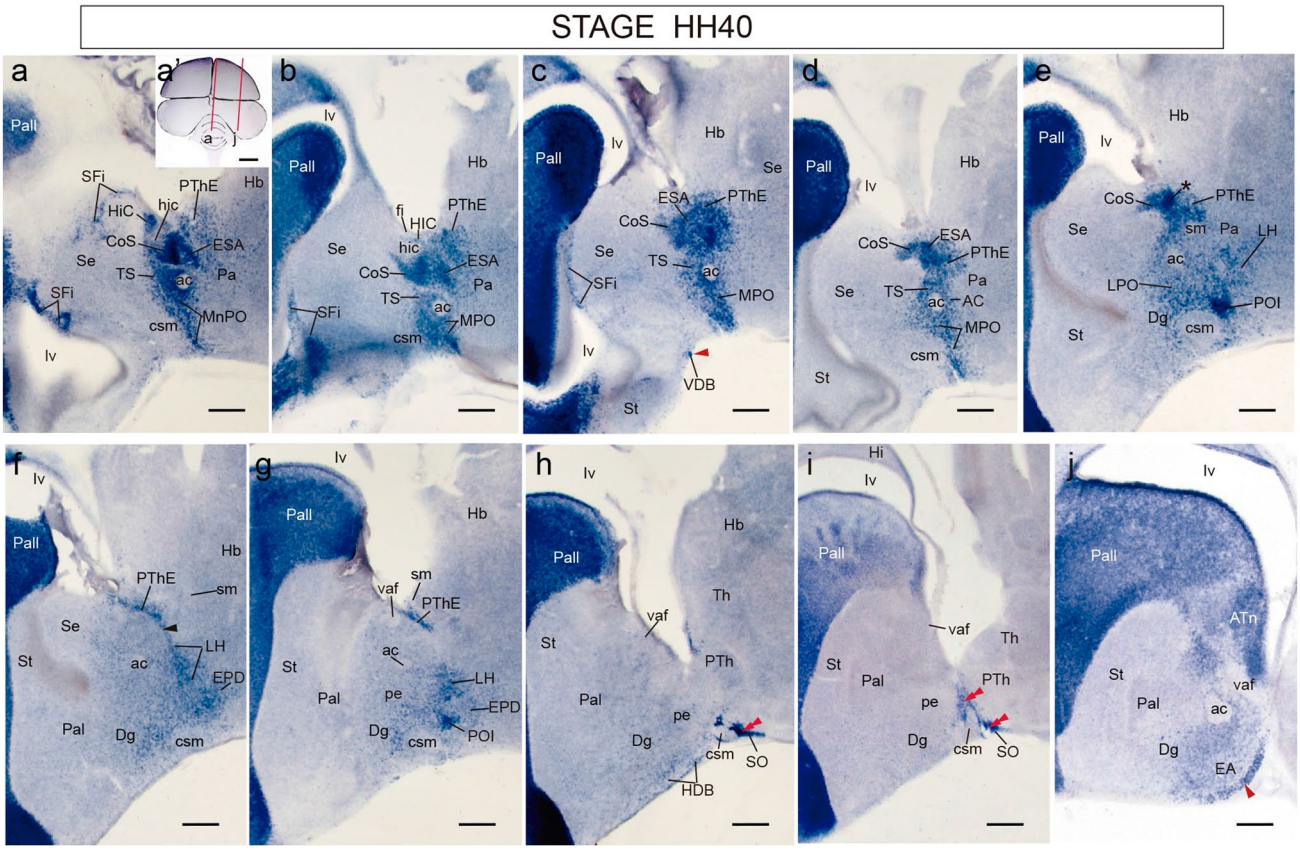

Fig. 9 *Tbr1* expression in the prosencephalon at stage HH40. **a–j** Mediolateral series of parasagittal sections through the rostral prosencephalon. Red arrowhead in **j** points to the telencephalic remnants of the peripeduncular migratory stream. The inset **a′** is a drawing showing the mediolateral range of sagittal sections shown in this series. Red double arrowheads in **h**–**i** point to the hypothalamic derivatives of the peripeduncular migration. Black asterisks in **d**, **e** indicate the caudal tip of the eminentio-septal area (ESA). Scale bars in **a**–**j**, 500 µm, and in **a′**, 5 mm

compact dorsally, where it lies deep to the peduncle (LH; Figs. 6a–c, 7g–j), but more ventrally it expands gradually into the topologically superficial peduncular tract. Here we noted a small hypothalamic extension parallel to the peduncle, and a small entopeduncular population. The latter represents the *Tbr1*-positive dorsal entopeduncular nucleus (EPD; Figs. 6a, b, 7k–m). Diverging rostromedially from this locus, other migrated juxtapeduncular elements enter the terminal hypothalamus, approaching the neighbouring lateral preoptic area. A number of cells of this more rostral juxtapeduncular stream soon arch medialwards in the direction of the medial preoptic area and the related anterior commissure. At this inflexion there appears the dense previously unknown aggregate named above the preoptic island (POI; Figs. 6d, 7k–m).

Stage HH40 (14 d.i.o.)

We illustrate what may be the final state of development of PThE derivatives at HH40 (14 days of incubation; i.e., 1 week before hatching), using oblique coronal sections (Fig. 8); this section plane seems intermediate between standard coronal and horizontal orientations, but is strictly topologically horizontal relative to the rostral diencephalon and the hypothalamus, i.e., parallel to the optic tract (schema in Fig. 8j). This plane is truly orthogonal to the peduncular tract as it courses within the peduncular hypothalamus, just rostrally to the prethalamus (pe; Fig. 8a–c). We will compare as well standard sagittal and horizontal sections at this stage (Figs. 9, 10). Generalities described for stage HH37 on the overall topography of the PThE relative to the laterally displaced amygdalo-hippocampal posterior (temporal) pole of the hemisphere and the new eminential relationships with various subpallial domains including the commissural septum remain valid.

The four caudalmost coronal sections show extratelencephalic elements of the whole thalamo-prethalamic alar complex (e.g., Hb, Th), featuring as well the PThE, which is now visible as a somewhat flocculent, well-delimited deep composite of weakly *Tbr1*-positive and negative cell patches. Remarkably, it lacks in general periventricular level

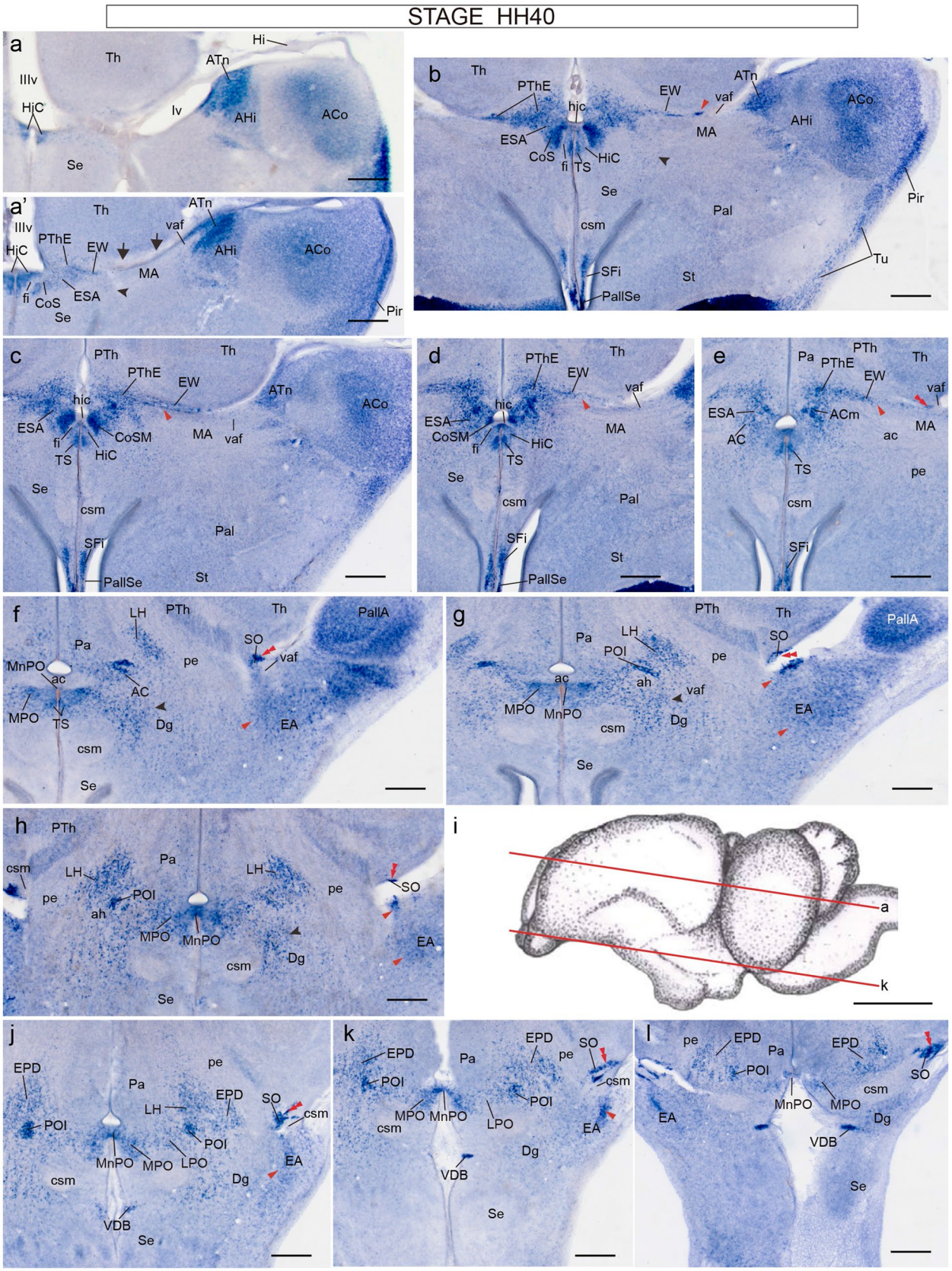
STAGE HH40
a
Hi
Th
ATn
IIIv
HiC
Iv
AHi
ACo
Se
a'
Th
ATn
IIIv
PThE
vaf
HiC
EW
AHi
ACo
MA
fi
CoS
ESA
Se
Pir
b
Th
PThE
hic
EW
vaf
ATn
ACo
ESA
CoS
fi
TS
HiC
MA
AHi
Se
Pir
csm
Pal
Tu
SFi
St
PallSe
c
PTh
Th
PThE
EW
ATn
hic
ACo
ESA
fi
CoSM
MA
vaf
TS
HiC
Se
csm
Pal
SFi
PallSe
St
d
PThE
Th
EW
vaf
hic
ESA
CoSM
MA
fi
HiC
TS
Se
csm
Pal
SFi
St
PallSe
e
Pa
PTh
PThE
Th
EW
vaf
ESA
ACm
AC
MA
ac
TS
pe
csm
SFi
f
LH
PTh
Th
PallA
Pa
SO
MnPO
pe
vaf
ac
AC
MPO
TS
Dg
EA
csm
Se
g
PTh
Th
PallA
Pa
LH
SO
POI
pe
ac
ah
vaf
MPO
MnPO
EA
csm
Dg
Se
h
PTh
csm
Pa
LH
LH
pe
pe
SO
POI
ah
MPO
MnPO
EA
csm
Dg
Se
i
a
k
j
EPD
pe
Pa
EPD
SO
LH
csm
POI
POI
MnPO
MPO
LPO
EA
csm
Dg
VDB
Se
k
EPD
EPD
SO
Pa
pe
POI
csm
MPO
MnPO
POI
csm
LPO
EA
Dg
VDB
Se
l
pe
EPD
Pa
EPD
POI
SO
csm
MnPO
MPO
EA
Dg
VDB
Se

◂**Fig. 10** *Tbr1*expression in the prosencephalon at stage HH40. **a–k** Dorsoventral series of horizontal sections through the rostral prosencephalon. **k′** Schema of an HH40 embryonic brain, illustrating the plane of the sections shown in **a–k**. Red arrowheads in **b–k** point to the telencephalic remnants of the peripeduncular migratory stream. Red double arrowheads in **e–l** point to the hypothalamic derivatives of the peripeduncular migration. Black arrowheads in **a′–b** and **f–h** point to juxtapeduncular migrated cells dispersed in the diagonal area (Dg). Scale bars in **a–k**, 500 µm, and in **k′**, 5 mm

representation of labelled cells, and has practically lost its former ventricular relief (PThE; Figs. 8a-d, 9a–g, 10a′, b–e). In contrast, the eminential complex remains connected laterally with the stretched rest of the peripeduncular migratory stream (red arrowheads), whose remnants can now be assumed to be fixed positionally. We suggest calling 'eminential wings' these eminential populations approaching bilaterally the caudal aspect of the peduncle (EW; Figs. 8b, c, 10a–e). The subpial aspect of the peduncle is now practically devoid of migrating peripeduncular cells, though some small subpial patches can be seen distal to the stream's origin (e.g., red arrowheads and double red arrowheads; Figs. 8b, c, 10e). As noted before, the extratelencephalic component of this stream (double red arrowheads) stabilizes in the area of the supraoptic nucleus (SO; Figs. 8a–c, 10f–h), while the telencephalic component ends in the extended amygdala (EA; Figs. 8e–i, 10f–h), after leaving midways a number of cells that penetrate medialwards the lateral, medial and median preoptic areas (LPO, MPO, MnPO; Figs. 8e–h, 10j–l), as well as other cells further along the telencephalic stalk that enter the subpial diagonal band formation. A distinct compact cell group forms within the vertical diagonal band nucleus (VDB; Figs. 9c, 10j–l). There is also a dispersed weakly labelled population which occupies the innominate area of the Dg subpallium surrounding caudally and laterally the cortico-septo-mesencephalic tract (Dg; csm; Figs. 8g–i, 9e–g, 10f–l); the latter diverges lateral- and caudalwards under the marginal septal and preoptic areas, to access the dorsolateral diencephalic surface in its descending path to the midbrain tectum (not shown). The topographic position of the relatively dispersed HDB and the VDB labelled elements is just rostral to this tract, as seen in sagittal and horizontal sections (see VDB, csm; Figs. 8i, 9c, h, 10j–l).

Passing now to derivatives of the juxtapeduncular migratory stream, the para-paraventricular lateral hypothalamic area (LH) displays a well-delimited *Tbr1*-positive population at intermediate mantle levels, deep to the peduncle (pe) and superficial to the paraventricular hypothalamic nucleus (Pa), which remains itself largelly unlabelled, though it also appears slightly flocculent, due to some weakly labelled neurons maybe dispersed from the neighbouring PThE (Pa; Fig. 8a–d). The LH leads ventrolaterally into the dorsal entopeduncular nucleus (LH, EPD; Figs. 8a–d, 9e–g, 10f–l). We still see medially to the EPD the small dense mass we tentatively named 'preoptic island'(POI; Figs. 8c, d, 9e, g, 10g–l).

Finally, the stabilized derivatives of the eminentio-septal migratory stream form a continuous periventricular bridge passing under the interventricular foramen between the alar PThE in p3 and the telencephalic septocommissural alar/roof region in hp1 and hp2 (hippocampal and anterior commissures, respectively; hic, ac). The bridging cells, interpreted not to be motile any longer at this stage (i.e., we think they initiated, but did not finish the migration), can be identified tentatively as an interposed eminentio-septal area (ESA). They generally form a denser population than the PThE proper (ESA; Figs. 8c–h, 9a–d, 10a–e; this cell group was not identified previously by Goodson et al. 2004; Puelles et al. 2007, 2019; Puelles 2018, or any other source). The ESA seems to contact at its rostral end the nucleus of the anterior commissure, which supposedly represents the entrance point of the eminentio-septal stream into the septocommissural region (AC; Figs. 8e–g, 10e, f).

The eminential cells migrated into the caudalmost septocommissural area are found in the neighbourhood of the hippocampal commissure. They essentially include the median nucleus of the hippocampal commissure (HiC), the triangular septal nucleus (TS), and the paramedian commissural septal nucleus (CoS); the latter may be divided into connected medial and lateral parts, ovoid in shape, which resolve rostrally into a laterally tapering wing, which points to the medial amygdala (HiC, CoSM, CoSL and red asterisk for the CoS wing; Figs. 8d–h, 9a–e, 10a–d).

The HiC (Figs. 8g, h, 9a, b, 10a–d) lies medial to the CoS and can be subdivided into a thin median portion that accompanies the hippocampal commissural fibres across the midline (see HiC; Figs. 8g, 9b), and two lateral ovoid portions, which are separated by the interhemispheric fissure, and limited laterally by the fimbrial tract as it approaches the commissure (HiC, fi; Figs. 8h, 9a; compare Puelles et al. 2007; Puelles 2018; atlas plate 15). It is possible that the HiC, and particularly its bilateral ovoid parts, receive *Tbr1*-positive cells from the pallial septum (Figs. 3p–r, 5a–i). It is therefore uncertain whether the eminentio-septal stream actually contributes to this nucleus.

Horizontal sections show that the bilateral HiC masses limit rostrally with the triangular septal nucleus, which extends along the commissural septum down to levels through the anterior commissure (TS; Figs. 8f–i, 9a–d, 10b–f). The TS appears itself in continuity with the bilateral bands of labelled cells located along the superficial medial preoptic region, caudally to the csm tract, at both sides of the paramedian preoptic nucleus (TS, MPO, MnPO, ac, csm; Figs. 8f–i, 9a–d, 10b–f).

Other derivatives of the eminentio-septal migratory stream penetrate the hp2 portion of the septum, where they associate with the anterior commissure (the latter

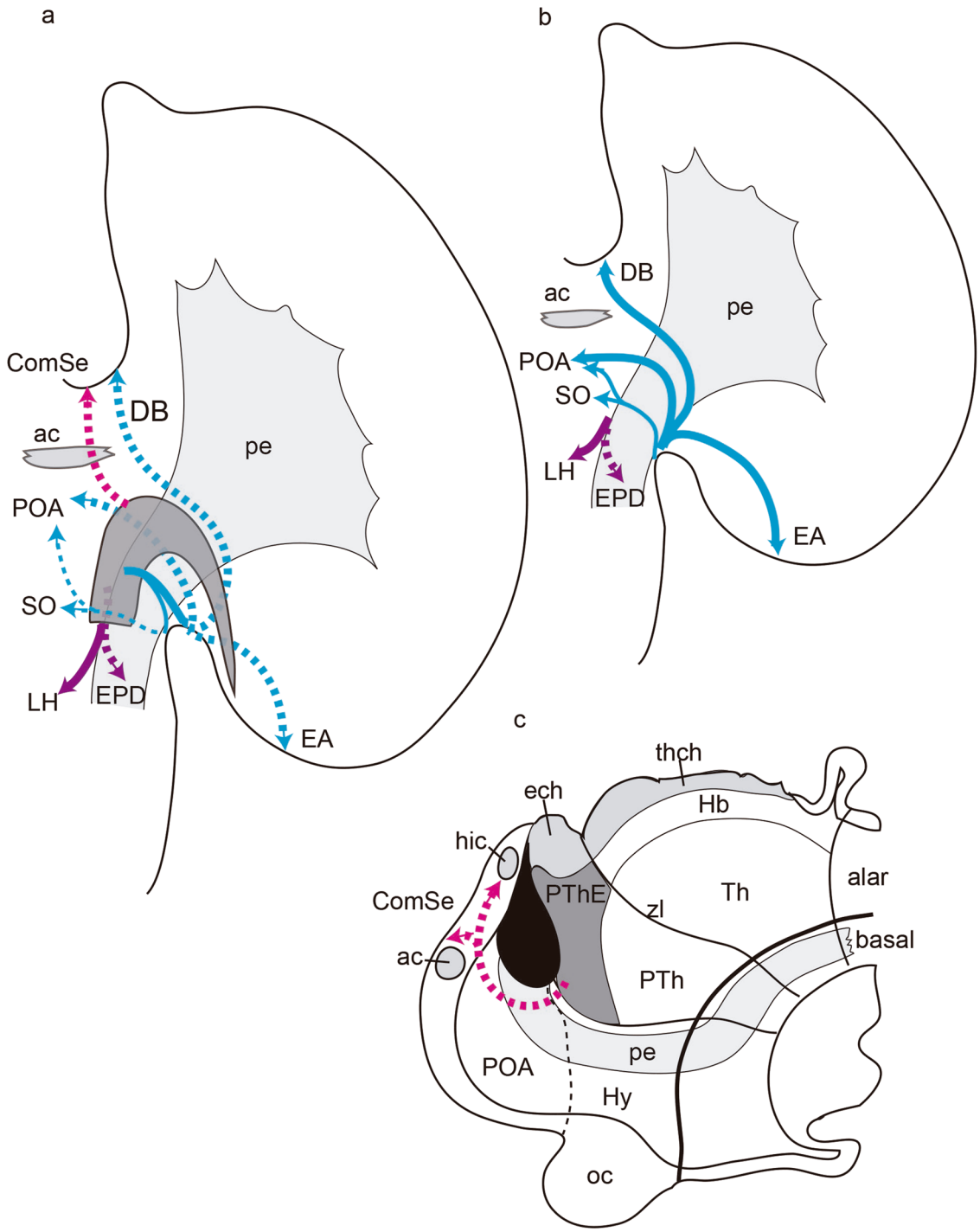

was fate-mapped in the chick as the rostral end of the neural roof plate; Cobos et al. 2001). The nucleus of the anterior commissure is formed bilaterally at the backside of the commissure (AC; Figs. 8f, g, 9d, 10f).

Discussion

Our results show that between the first and second week of incubation of chick embryos there occur remarkable changes in the distribution of *Tbr1-expressing* cell populations in the area containing the prethalamic eminence and its surroundings. The PThE itself, which is initially massively labelled, gets progressively reduced to an interstitial or bed nucleus

◂**Fig. 11** Diagrams summarizing the conclusions drawn about the eminential migration streams. **a** The telencephalon and neighboring forebrain are represented here as seen from above and rendered transparent, to visualize schematically the PThE as a bent and tapering dark gray mass extending partly into the medial wall of the evaginated hemisphere. Other relevant landmarks entered are the peduncle (pe; light gray), passing underneath the eminentia into the hypothalamus, and the anterior commissure (ac; light gray), which indicates the transition between the preoptic area (POA) and the commissural septum (ComSe). The three eminential migrations are color-coded. The peripeduncular stream is represented in blue color; it sorts out of the PThE in lateral direction, passes subpially over the peduncle and divides into thick telencephalic and thin extratelencephalic components (non-dashed portion of the blue trace, visualized on top of the peduncle). As the cells migrate around the peduncle they spiral variously into telencephalic territory (dashed blue traces), dividing into separate streams that reach the extended amygdala (EA), the preoptic area (POA), the diagonal band nuclei (DB) and, via the extratelencephalic component, into the supraoptic nucleus (SO) and the preoptic area (POA). All of them advance subpially, but on the underside of the area visualized in this schema, seen by transparency (dashed traces). The juxtapeduncular stream is represented in mauve color. It descends in the intermediate stratum from the PThE into the medial aspect of the peduncle to reach the lateral hypothalamus (LH); some cells penetrate the peduncle and form there the dorsal entopeduncular nucleus (EPD; dashed mauve trace). Finally, the eminentio-septal stream is shown in red color. The cells contour in an arch the interventricular foramen (see **c**), pass behind the anterior commissure (ac) and enter the commissural septum, advancing therein into the hippocampal commissure (not shown in **a**, but see **c**). **b** This schema visualizes the hemisphere and peduncle as seen from the ventral forebrain surface (i.e., viewpoint opposite the perspective in **a**, and, implicitly, the contralateral hemisphere). The peripeduncular stream (blue trace) and the juxtapeduncular stream (mauve trace) are accordingly seen directly as they approach EA, DB, POA, SO and LH (therefore, no dashes), after sorting the peduncle on its lateral or medial aspects, respectively. Only the juxtapeduncular cells entering the EPD are seen by transparency (dashed mauve trace). **c** This schema represents the right half of the rostral diencephalon (thalamus, Th, and prethalamus, PTh) and hypothalamus (Hy), visualizing the ventricular surface through a median sagittal section. The interprosomeric boundaries of Th and PTh, including the interthalamic zona limitans (zl), are seen as transversal lines extending from roof to floor, crossing orthogonally the alar-basal boundary (thicker longitudinal black line; see also 'alar' and 'basal' at right). The hypothalamo-telencephalic boundary (or hypothalamo-preoptic limit) is indicated by a black dash-line. The interventricular foramen is drawn as a black surface which receives through the underlying hypothalamus (Hy) the peduncular tract (Pe; light gray). The foramen is limited caudally by the PThE, which bulges into it where it bends into its evaginated tapering portion (compare bent shape of PThE in **a**). The PThE is shaded in dark gray. It occupies an extreme dorsal position within alar PTh, and displays dorsally the taenial attachment of the prethalamic or eminential chorioidal roof plate (ech); the latter is caudally continuous with the thalamic analogue (thch) (both ech and thch in light gray). Other markings include the habenular area (Hb), the optic chiasma (oc), the preoptic area (POA), the anterior commissure (ac), the hippocampal commissure (hic) and the commissural septum (ComSe). The periventricular course of the eminentio-septal stream is represented as a red dashed trace extending along the hemispheric stalk into the septal commissural roof plate (ComSe), thus expanding the visual image of this stream given in **a**. This course is held to be restricted to the evaginated telencephalon, eschewing the POA territory (this refers to distinct prosomeres hp1—where the migration occurs in relation with the peduncle—and hp2—containing the eschewed POA—these prosomeric units were not represented explicitly for reasons of simplicity)

of the stria medullaris (BSM). This tract carries fibres from the basal forebrain, septum, preoptic area and hypothalamus (lateral hypothalamus and the dorsal entopeduncular nucleus), which target the PThE itself. It transits longitudinally across the PThE and then ends at the thalamic habenular region, or crosses the habenular commissure (Díaz and Puelles 1992a). Accompanying the differentiation of the BSM at the PThE locus, numerous surrounding structures which initially did not contain *Tbr1*-positive cells acquire such elements, in some cases quite massively. This pattern might be understood in principle as due to delayed independent expression of this marker at the diverse emergent sites, but this interpretation is contradicted by our staged sequences of histological images, which are consistent instead with the alternative notion that many labelled cells originate at the PThE and stream via three well-defined tangential migration pathways into the surrounding territories. Some eminential derivatives apparently stabilize at intermediate points along these pathways, establishing bridges of labelled cells between the PThE and neighbouring hypothalamic and telencephalic regions (Fig. 11).

The migratory interpretation of these phenomena clearly needs caution, given the existence of alternative potential *Tbr1*-positive sources at least for some of the hypothetically migrating contingents (e.g., pallial septum, pallial amygdala, or other parts of telencephalic pallium). There is experimental evidence that some pallial neurons migrate tangentially into the subpallium (e.g., Striedter et al. 1998). We also saw images consistent with that phenomenon, but these are distant and can be separated from the apparent eminential migrations. On the other hand, Watanabe et al. (2018) reported recently experiments revealing an eminential origin of two mouse septal nuclei (the bed nucleus of the anterior commissure and the triangular septal nucleus). Experimental testing and corroboration of any migratory hypothesis is obviously appropriate.

It so happens that our analysis of this chick brain region started as an experimental fate-mapping approach (thesis work of A.A.), but the unsystematised anatomic complexity of the apparent derivatives of the PThE in scarcely understood surrounding forebrain parts (further complicated by considerable undescribed morphogenetic deformation of the telencephalic stalk area) rendered both the description and interpretation of experimental results very difficult. We thus turned to the present preliminary and strictly descriptive longitudinal mode of analysis of this Cinderella-like brain region, an endeavour made possible by the relative selectivity of the *Tbr1* marker for eminential cells and the peculiar position of the PThE (Fig. 11a, c). This allowed us to recognize and systematize the three different migratory routes, following individually the respective progressive changes to produce an overall model of the postulated PThE migratory phenomena (Fig. 11a–c). We threw light in

this process on some anatomic issues that were previously unclear in the existing literature. Such results did not seem reducible to a brief anatomic introduction within our report of experimental results. Their publication in full was deemed to be of interest, since there are very few published data on the development of the avian (or any other) PThE. We present here this analysis, drawing only provisional conclusions as regards the postulated migrations, reaching only as far as these can be supported by sequential descriptive data in three section planes, and pending ulterior corroboration by our existing experimental results, whose presentation and interpretation indeed results much simplified by the availability of a preliminary developmental anatomic model.

The PThE as an anatomic and developmental unit.

At early stages up to HH25-26 (Fig. 1) the chicken prethalamic eminence (PThE) constitutes a well-defined dorsal alar domain of the diencephalic prethalamus (in fact, the dorsalmost prethalamic area; Puelles et al. 2007, 2019; Puelles 2018; Fig. 11c). It displays in both the chick and the mouse a singular molecular profile that distinguishes it from the rest of the prethalamic alar plate. It does not express *Dlx* genes (and therefore does not produce GABAergic neurons), and expresses instead gene markers consistent with the local generation of glutamatergic neurons (*Pax6* in the ventricular zone, *Tbr2* in the subventricular zone, and *Calb2*, *Tbr1, Lhx5, Trp73, Grm1, vGlut2, Tfap2a, Gdf10,* and *Lhx9* in the mantle zone (Abbott and Jacobowitz 1999; Puelles et al. 2000, 2012; Abellán et al. 2010a; Shimogori et al. 2010; Ruiz-Reig et al. 2017, 2018). This eminential prethalamic area is often misidentified in the literature as 'thalamic eminence'. This obsolete usage refers to an old terminology coming from historic periods in which it was not yet recognized that the 'thalamus' shows embryonic and adult subdivisions into parts now generally recognized as 'thalamus' (old 'dorsal thalamus') and 'prethalamus' (old 'ventral thalamus') (Puelles and Rubenstein 2003). Once this fundamental subdivision is accepted, and the zona limitans intrathalamica of Rendahl (1924) is acknowledged as the intervening transversal boundary [Puelles 2018; zl in Fig. 11c; incidentally, the zl also serves as the local secondary organizer for rostrocaudal pattern; see Puelles and Martínez (2013)], the eminentia clearly turns out to be prethalamic.

Using the prosomeric forebrain model as a descriptive background (Puelles et al 2000, 2012; Puelles and Rubenstein 2003, 2015), the PThE has a dorsal taenial border where the corresponding prethalamic part of the diencephalic chorioidal tela attaches (prethalamic or eminential taenia; Figs. 1, 11c; see Puelles 2019). The PThE initially contacts rostrally the hypothalamic paraventricular area, as well as the caudal poles of the evaginated amygdalar and hippocampal pallial areas of the telencephalic hemisphere. While an eminential contact with the pallial amygdala and the caudal hippocampus is evident early on (this contact occurs underneath the prospective chorioidal fissure of the lateral ventricle; Figs. 1, 2a, b, e, f; tapering part of PThE in Fig. 11a), subsequent disproportionate enlargement of the hemisphere causes the pallial amygdala and the hippocampus to be pulled apart from the PThE, so that at more advanced stages it seems to have portions of the subpallium as closest neighbours, including the medial amygdala (Fig. 3k). It becomes increasingly unclear whether a stretched eminentio-amygdalo-pallial contact territory persists in a cryptic form at the bottom of the terminal sulcus.

The PThE participates variously in the process of telencephalic evagination [depending on the species, and more so in mammals (Puelles et al. 2000) than in birds; present results; Figs. 2, 3, 4, 11a]. In the chicken case a small rostrodorsal part of the PThE forms a neuroepithelial flap that appears deflected into the posteromedial wall of the hemisphere (carrying with it roof-derived chorioidal tissue transitional between prethalamus and telencephalon; Puelles 2019). The resulting bent ventricular surface of the PThE generates a markedly protruding bulge at the back of the interventricular foramen. This bulge is what originally inspired the classical Latin descriptor 'eminentia thalami' (i.e., the 'thalamic bulge'; see Figs. 2b, e, f, 3b, i, n, 4d, 11a, c). However, in the chick the major part of the PThE remains within the diencephalic wall, immediately caudal to the interventricular foramen.

The PThE limits caudally (across the zona limitans boundary) with the thalamic habenular area (Hb; Fig. 11c), which is a similarly hyperdorsal, roof-contacting area within the thalamus. The stria medullaris tract courses longitudinally in sequence across the dorsal alar hypothalamus, the PThE and the habenula, extracting fibre components from hypothalamic and eminential bed nuclei of the stria medullaris which target the habenula (Díaz and Puelles 1992a; Puelles et al. 2012).

It might be tempting to conjecture that the PThE, given its molecular profile, which is similar in several aspects to the initially continuous telencephalic pallium, represents an ectopic, extratelencephalic part of the pallium (this point is still under discussion in the case of lampreys, or agnathans; see Pombal and Puelles 1999). One observation that discrepates with this notion (present results) is that the PThE does not express the telencephalic marker *Foxg1*, though this also occurs in part of the mouse hippocampus (Xuan et al. 1995; Shimogori et al. 2010; Kumamoto and Hanashima 2017; Watanabe et al. 2018).

While the PThE is clearly identifiable anatomically and molecularly in embryos (Fig. 1), it apparently becomes reduced in relative size, and is rather cryptic at advanced embryonic stages, particularly so after hatching in the chick, but also in mammals. Indeed, some authors have held the

PThE represents a transient anatomic structure (commented by Watanabe et al. 2018). Standard atlases of the brain of rodents or birds usually do not identify a PThE, though they may illustrate the bed nucleus of the stria medullaris without clarifying its prethalamic ascription (BSM; e.g., Paxinos and Watson 2014). The avian PThE is nevertheless identified in a recent chick brain atlas (Puelles et al. 2007, 2019).

We have used the pervasive expression of *Tbr1* mRNA observed within the eminential mantle layer at early embryonic stages (Fig. 1a) to examine in detail the histogenetic evolution of this little understood prethalamic formation. It turns out that the progressive late-embryonic reduction in visibility of the PThE is accompanied by appearance of various other *Tbr1*-positive cell populations in the rostral forebrain, all of which tend to remain connected by *Tbr1*-labelled cell bridges with the PThE. This pattern is suggestive of at least three distinct routes of tangential migration of eminential neurons expressing *Tbr1*, using respectively deep, intermediate and marginal strata of the mantle layer. These apparently migrating populations all invade in topological rostralward direction neighbouring hypothalamic and telencephalic areas (Fig. 11a–c), but some derivatives stop at intermediate positions along these pathways, establishing persistent bridges.

The apparent migratory routes and eminential derivatives classified by migration route.

Correlative histological images suggestive of *Tbr1*-labelled cell populations emerging from the PThE and penetrating neighbouring forebrain territories illustrate three distinct phenomena called by us the peripeduncular, juxtapeduncular and eminentio-septal migratory streams (Fig. 11). The peripeduncular and juxtapeduncular streams can be distinguished already in HH25-26 embryos as a joint advancing front, in presence of a barely incipient peduncle (Fig. 2a, b). As the peduncle enlarges subsequently, it separates a subpial (marginal) peripeduncular component from an intermediate juxtapeduncular component (deep to the peduncle; Fig. 11a, b). Later, a deep subpopulation of the PThE migrates separately (always periventricularly) under and in front of the interventricular foramen and thereafter enters the septo-commissural area, representing our eminentio-septal stream (Fig. 11c). We also found evidence of an independent *Tbr1*-positive septo-commissural tangential migration originated in the pallial septum (Puelles et al. 2000). All three eminential streams advance first rostrally into the hypothalamus, before entering the overlying telencephalon and diverging into different target territories in telencephalon or hypothalamus.

1. The peripeduncular stream crosses subpially the transverse hypothalamo-prethalamic boundary and penetrates the marginal stratum of the hypothalamic paraventricular area, which lies immediately rostral to the PThE, coursing therein rostralward and subpially around the peduncle (note the peduncle courses dorsoventrally through the superficial stratum of the peduncular hypothalamus, as interpreted in the prosomeric model; Puelles et al. 2012; Puelles and Rubenstein 2015). This voluminous migratory stream includes *telencephalic* and *extratelencephalic* sections (Fig. 11a, b): after surpassing the peduncular obstacle, the dorsalmost cell population advances in an oblique spiral into the telencephalon. These cells remain subpial, and one of their targets is the extended amygdala, while others are diverted before from that route either by entering into the diagonal band, or into the preoptic area. In the last case, labelled cells proceed subpially across the lateral and medial preoptic areas, and reach finally the median preoptic nucleus, located rostrally to the anterior commissure. The latter group, as well as cells coursing through the diagonal band, contribute also to dispersed cells in the innominate area (surrounding the cortico-septo-mesencephalic tract at the base of the septum). In contrast, the extratelencephalic peripeduncular migrating elements remain within the marginal hypothalamus (paraventricular area). Once past the peduncle, they enter the terminal hypothalamus, and end superficially in the characteristic neighbourhood of the supraoptic nucleus (Fig. 11a, b).

As development advances, our results show that the number of cells forming the peripeduncular stream gradually diminishes (coinciding with the increase in labelled cells at the target territories), but there always remains a stretched proximal or bridge contingent that becomes definitively stabilized in contact with the PThE, forming what we called the ‘eminential wings’.

Abellán et al. (2010a) and Vicario et al. (2017), describing expression of *Lhx* genes in mouse, chicken and zebra finch embryos, observed eminential *Lhx5*-positive cells apparently migrating around the cerebral peduncle (our peripeduncular stream), and entering the medial extended amygdala territory (Abellán et al. 2010a; their Fig. 1f, 5b, e, 8a–c). Vicario et al. (2017) showed further zebra finch *Lhx5* labelling, where labelled peri- and juxtapeduncular migratory streams coming out of the PThE can be clearly identified (their Fig. 6c). Bulfone et al. (1995) found *Tbr1*-positive cells within the mouse diagonal band nuclei, which were thought to be probably migrated, but without postulating the prethalamic eminence as their potential source. Puelles et al. (2000) observed chicken *Tbr1*-positive cells in the shape of the peripeduncular stream (at 8 d.i.o.; their Fig. 8b), as well as in places we would now interpret as the extended amygdala and the septo-commissural area (at 10 d.i.o; their Fig. 9j, labelled as DBH

and DBV, respectively). Cabrera-Socorro et al. (2007) showed an image consistent with a peripeduncular eminential migratory stream in a lizard (their Fig. 3d).

2. The juxtapeduncular stream also invades the hypothalamic paraventricular area, but penetrates it at intermediate levels of the mantle layer, through the local 'lateral hypothalamus' tier (site of the medial forebrain bundle, deep to the peduncle; Puelles et al. 2012); accordingly, its major cell population advances, and partly becomes fixed, deep to the peduncle. This population may correspond to that named prereticular lateral hypothalamic nucleus in the mouse (Puelles et al. 2012); the aim in that prosomeric study was to classify molecularly distinct dorsoventral components of the classic lateral hypothalamus across the basal and alar domains of the hypothalamus; we presently confirm that the chicken also has a *Tbr1*-positive prereticular lateral hypothalamic nucleus. This population is found within the peduncular hypothalamus (PHy), just superficially to the main mass of the paraventricular nucleus, which remains *Tbr1*-negative itself (this cell group also appears labelled selectively with *Lhx5*, another eminential marker, in Vicario et al. 2017; their Fig. 6c). A smaller and topologically more superficial contingent of this stream penetrates the peduncle interstitially and forms therein the dorsal entopeduncular nucleus (this is homologous to the mammalian counterpart, which is also *Tbr1*-positive; Wallace et al. 2017; Puelles et al. 2012 and unpublished observations). Having passed deep to the peduncle, the juxtapeduncular stream ends within the terminal hypothalamus (THy) and the associated preoptic area. At this point another subgroup of its neurons—named by us provisionally the 'preoptic island'—coalesces in the neighbourhood of a fibre tract. Previous analysis of this area in the mouse (Puelles et al. 2012) indicated the existence of a hypothalamic bed nucleus of the stria medullaris (hBSM) divided into terminal and peduncular moieties. These formations lie just under the preopto-hypothalamic border, a locus that is consistent with that of the 'preoptic island'. It is credible that part of the eminential neurons migrated under the peduncle into the chicken hypothalamus may constitute an avian hypothalamic BSM nucleus, which presumably projects to the habenula via the stria medullaris tract.
3. The eminentio-septal stream represents another *Tbr1*-positive cell population exiting the PThE in rostral direction (Fig. 11a, c). It becomes visible later than the two other streams (it was first observed clearly at stage HH33; 8 d.i.o.), and courses periventricularly rostralward under the interventricular foramen (traversing the dorsalmost alar hypothalamus before entering the telencephalon), and finally approaching the median septo-commissural region. It enters this region passing first behind the anterior commissure, and then progressing backwards towards the locus of the hippocampal (pallial) commissure. The main eminentio-septal stream derivatives finally lie at median and paramedian sites of the septal commissural plate, associated to the hippocampal commissure or to the anterior commissure. However, these septal elements remain connected with the PThE by a voluminous bridge of stabilized labelled cells (named by us the eminentio-septal area, or ESA), which occupies the compacted space in between. These septo-commissural target sites in the forebrain roof plate are found very close to the PThE at late-embryonic stages (Figs. 6, 7, 8, 9), but actually are quite distant topologically, since they are separated from the PThE by the prethalamo-telencephalic chorioidal roof plate (non-permissive for cell migrations), as well as by the whole evaginated hemisphere (Figs. 1a, b; 11c).

An identical calretinin-positive eminentio-septal cell migration has been recently demonstrated experimentally in the mouse by Watanabe et al. (2018). According to these authors, who did not name this migration, it gives rise to the bed nucleus of the anterior commissure and the triangular septal nucleus (a nucleus of the hippocampal commissure). These mouse eminential cells apparently follow a similar pathway under and in front of the interventricular foramen, though the authors did not describe it precisely. The apparent avian derivatives of the eminentio-septal stream likewise include a bed nucleus of the anterior commissure and a triangular septal nucleus, in addition to the nucleus of the hippocampal commissure and the commissural septal nucleus (HiC, CoS). The possible homologs of these other nuclei in mammals are unknown. Cabrera-Socorro et al. (2007) showed that the lizard HiC nucleus distinctly expresses *Tbr1* (their Fig. 6b). Hetzel (1974, 1975) concluded from his embryological studies in a lizard that the reptilian nucleus of the pallial commissure, a possible homolog of the triangular septal nucleus of birds and mammals, derives embryologically from the eminential region. This nucleus was found to project to the habenula in lizards (Díaz and Puelles 1992a; Font et al. 1998).

We show that the chicken CoS nucleus appears divided into medial and lateral parts. These two CoS parts were illustrated, but not distinguished or named, by Goodson et al. (2004) and Puelles et al. (2019). Incidentally, the newly published color images of the chick atlas reveal that CoS is largely formed by parvalbumin-positive cells, whose axons seem to course ipsilaterally via the ESA, the PThE and stria medullaris into the habenula; these neurons accordingly would not represent true commissural cells. Our present results add their *Tbr1*-positive typology, which possibly is related to a glutamatergic nature.

Importantly, though, we identified in the pallial septum a second potential source of *Tbr1*-positive septo-commissural neurons. We saw this apparent septo-septal or septo-commissural migration at stages HH33 and HH36, in the shape of distinct bilateral streams of labelled cells which sort out of the pallial septum, and traverse the unlabelled subpallial septum until they reach the area of the hippocampal commissure (Figs. 3u–w, 5a–i). These migrations seem to stop after HH36, leaving next to the septal pallio-subpallial boundary a string of labelled cell aggregates which we tentatively identified as the avian septo-fimbrial nucleus. Our data suggested that this septal migration might contribute mainly to the lateral HiC masses in the area of confluence with the eminentio-septal stream, but this point absolutely needs experimental corroboration.

Abellán et al. (2010a) illustrated chick embryo material showing expression of both *VGlut2* (at 12 d.i.o) and *Lhx5* (at 10 d.i.o) at similar bilateral septo-commissural streams, interpreting them not as a migration targeting the hippocampal commissure, but as an 'extension' of the pallial septum (their Figs. 4e, f, g, g′). The nucleus of the hippocampal commissure itself was shown by Abellán et al. (2010a) to express *Emx1* at 10 d.i.o. (their Fig. 4h); this marker is also shared by both the PThE and the pallial septum (LP—unpublished observations—observed likewise years ago a septo-commissural migration of *Emx1*-positive cells). Abellán et al. (2010a) further reported *Lhx1*-positive neurons at the chicken CoS (12 d.i.o.), but we think that what they identified as CoS is a non-commissural preoptic cell population lying adjacent to the anterior commissure; it does not agree in relative position with our concept of the CoS, always found next to the hippocampal commissure (Goodson et al. 2004; Puelles 2018).

Other eminential migrations postulated in the literature

Apart of reported evidence cited above, which corroborates the three eminential tangential migration streams we presently postulate (peripeduncular, juxtapeduncular and eminentio-septal), the literature contains as well other hypotheses about some long-range eminential migrations. We discuss them separately in this section because we did not find evidence for them in our *Tbr1*-reacted material. This does not mean we negate their existence, because it is well possible that *Tbr1* may not be an appropriate marker for their demonstration.

On one hand we have the hypothesis in mouse of a long-range migration of eminential cells into the accessory olfactory bulb, which reportedly shows characteristic expression of the *Ap2α, Lhx5, NP2* and *Tbr2* markers (Huilgol et al. 2013; review in Ruiz-Reig and Studer 2017). This cell stream proceeds rostralwards along a lateral pallial pathway that apparently coincides with the ventropallial lateral olfactory tract (lot). It is known that the lot has in many species a postamygdalar habenulo-commissural extension that circulates within the stria medullaris through the PThE. It would seem, accordingly, that this stream uses the topologically rostral border of the PThE with the pallial amygdala to enter a ventropallial course towards the accessory olfactory bulb, guided or not by the lot fibres. Given the deduced course through the ventral pallium (Puelles et al. 2016b), local pallial *Tbr1*-positive neurons would impede us recognizing this migration in our material (but we did not distinguish this contingent in our chick material either with *Tbr1* or with *Tbr2*). Birds seem to have lost evolutionarily the accessory olfactory bulb, and this might cause this migration to be absent in birds, if it depends on an attraction effect from its target, or on guidance via the accessory olfactory tract. Nevertheless, birds maintain a reduced olfactory tract putatively reaching the habenular commissure, so that rostralward guidance of this migration through the subpial ventral pallium might be assured if it depends on contact with the lot, even if final lack of target-derived trophism later leads to death of the migrated cells.

A second reported eminential migration we did not observe is that of 'lot' cells, that is, the so-called 'guidepost cells' of the lateral olfactory tract (Ruiz-Reig et al; 2016; Ruiz-Reig and Studer 2017). This migration is characterized molecularly by expressing selectively *mGluR1, Lhx5, Trt73, Grm1* and *Lot1*. Again in this case, the putative migration courses beyond the pallial amygdala through the ventral pallium.

A further long-range migration which is reported to originate partially in the PThE in reptiles and mammals is that of prethalamic Cajal–Retzius neurons (C-R); a contingent of such cells expressing *p73* (but being *reelin*-negative; see below) has been postulated to invade tangentially cortical layer 1, similarly as other C-R neurons do which come from various other sources around the cortex (Grove et al. 1998; Meyer and Goffinet 1998; Meyer and Wahle 1999; Meyer et al. 1999, 2002; Zecevic and Rakic 2001; Takiguchi-Hayashi et al. 2004; Bielle et al. 2005; Yoshida et al. 2006; Louvi et al. 2007; Imayoshi et al. 2008; Tissir et al. 2009; Abellán et al. 2010a,b; Griveau et al. 2010; Teissier et al. 2010; Zimmer et al. 2010; Meyer 2010; reviews in Pierani and Wassef 2009; Borello and Pierani 2010; Puelles 2011; Barber and Pierani 2016). Given that the PThE does not contact directly the dorsal pallium (the primordium of the neocortex; see Pattabiraman et al. 2014; Puelles et al. 2019), it remains unclear so far how the postulated eminential C-R cells would cross the outer allocortical ring, as well as the inner mesocortical ring, to reach the neocortex, or one of its sectors. Though there is clear evidence of *p73* expression at the PThE, the translocation of eminential *p73* cells into the cortex is insufficiently documented.

The image used by Cabrera-Socorro et al. (2007) to support the hypothetic spread of eminential *p73*-positive C-R cells into the hemisphere of a lizard is comparable to our chicken *Tbr1* material indicating partial evagination of the PThE into the telencephalic posterior wall, up to a contact with the caudal hippocampal cortex (their Fig. 1b; note lack of eminential *reelin* expression in their Fig. 1c). Tissir et al. (2009) mapped *DeltaNp73* mRNA in embryonic mice and concluded that the positive C-R cells do not originate from the PThE (identified as 'eminentia thalami'). These authors concluded that the observed *DeltaNp73*-positive neocortical C-R cells largely originate from the retrobulbar area and the cortical hem (fimbrial or hippocampal taenia); they also illustrated aggregates of *DeltaNp73*-positive elements at the site of the lot, and along the diagonal band (the latter detail would be consistent with our subgroup of peripeduncular cells arriving at the diagonal band nuclei).

Patterns of connectivity

It is remarkable that various putatively migrated PThE derivatives share a projection to the habenula, this being also a property of the non-migrated eminential BSM nucleus. These projections are largely grouped into those targeting the medial or the lateral habenula, with scarce examples of cell groups projecting to both targets.

As regards reptiles, in vitro HRP-labelling experiments restricted to the medial habenula of *Gallotia galloti* lizards produced retrograde labelling within the 'nucleus eminentiae thalami', i.e., the BSM, the nucleus of the posterior pallial commissure (an anatomic singularity of lizards), and the 'nucleus septalis impar' (a triangular septal nucleus homolog). Similar experiments on the lateral habenula caused retrograde HRP transport at the BAC, the DBH, the lateral preoptic area, the 'anterior entopeduncular nucleus' (corresponding to the dorsal entopeduncular nucleus of the present account), the lateral hypothalamic area (corresponding to our prereticular lateral hypothalamic nucleus), the lateral mamillary nucleus, and the nucleus of the stria medullaris (Díaz and Puelles 1992a). The sites mentioned which appear in italics (all except the mamillary body) correspond to loci where *Tbr1*-positive eminential derivatives were traced in the chick. Font et al. (1998) placed two control HRP injections in the habenula of the lizard *Podarcis hispanica*, and obtained retrograde transport at the nucleus of the posterior pallial commissure and their 'impar septal nucleus' (the latter may be compared in position to the triangular septal nucleus in birds and mammals).

In mammals, habenular afferences were studied in detail in the rat by means of retrograde HRP transport by Herkenham and Nauta (1977). They found that label deposited at the medial habenula was transported selectively to the entopeduncular nucleus and neighbouring lateral hypothalamus, with minor labelling of the local perifornical nucleus, and the lateral preoptic area. Their illustrations show that the labelled EP, LH and PFx neurons are found precisely at levels through the paraventricular hypothalamic nucleus, as we would predict if they relate to the juxtapeduncular migration stream. Moreover, there is abundant evidence that a dorsal component of the mouse, rat and monkey entopeduncular nucleus projects differentially to the lateral habenula, whereas the neighbouring ventral entopeduncular component projects to the thalamus (Nauta 1974; Herkenham and Nauta 1977; Carter and Fibiger 1978; Parent 1979, 1986; Parent et al. 1981, 1984; van der Kooy and Carter 1981; Parent and De Bellefeuille 1982; Namboodiri et al. 2016; Zahm and Root 2017). This result was recently verified with modern optogenetic methodology by Wallace et al (2017).

In the monkey (e.g., Parent 1986), the presumptive 'entopeduncular' habenulopetal neurons were identified ventromedially to the thalamopetal neurons found in the primate internal pallidal segment (which is widely assumed to lie within the telencephalon). However, the habenulopetal cells invaded the cerebral peduncle, that is, had an entopeduncular hypothalamic topography, suggesting against the dogma we see in the literature that monkeys (not only rodents) also have entopeduncular nuclei, apart of having two pallidal portions (external and internal). One probably can now expect generally in mammals two telencephalic pallidal centers (see Silberberg et al. 2016) and at least two different hypothalamic entopeduncular formations, according to the circuitry shown by Wallace et al. (2017) in mice. This allows an updating of the standard comparative model of the basal ganglia circuit in rodents and primates.

More sporadically, the lateral habenula experiments of Herkenham and Nauta (1977) labelled also dispersed cells within the 'magnocellular basal forebrain'. This included the diagonal band, substantia innominata and basal nucleus of Meynert, all of which are modernly ascribed to the diagonal subpallial area (Puelles et al. 2013, 2016a), also related to the 'extended amygdala' concept of Heimer and colleagues used by us in the chick (de Olmos and Heimer 1999). Some such cells were also observed contralaterally. Remarkably, Abellán et al. (2010a) show considerable expression of *VGlut2* (the glutamatergic marker) in the avian extended amygdala, characterizing it as a 'pallial extended amygdala' (EAp in their Figs. 4e, 6f, 8e). This category was first proposed in the Puelles et al. (2007) chick brain atlas; otherwise, Heimer's original concept of the extended amygdala requires subpallial characteristics. In the present context, we think that this avian para-amygdalar *VGlut2* expression is probably due to the eminential origin of many cells in this area, rather than to a pallial origin. Nevertheless, our descriptive analysis is not able to support strongly enough this hypothesis.

The crossed 'basal forebrain' habenulopetal elements of Herkenham and Nauta (1977) could not be confirmed in our chick material. Interestingly, they may be due to a singularity of mammals represented by the median fusion of the septal halves across the primary interhemispheric fissure. This fusion in principle would allow eminential cells migrating along the diagonal band to pass contralaterally, eventually carrying passively elongating axons with them. Alternatively, some cells migrated only ipsilaterally can send their axons across the fused median septum into the contralateral stria medullaris and habenula (but neither birds nor reptiles display a septal median fusion; see Fig. 10). Such sparser labelled basal forebrain elements agree with the distribution of some of our telencephalic peripeduncular eminential migratory cells.

Alonso et al. (1986) interestingly described anterograde transport of autoradiographic label from the rat supraoptic nucleus (SO) into the lateral habenula. This source may represent the extratelencephalic eminential peripeduncular subpopulation which targets the supraoptic nucleus, whose main hypophysotropic population surely is of hypothalamic paraventricular origin.

On the other hand, Herkenham and Nauta (1977) found that HRP deposits restricted to the medial habenula labelled mainly septocommissural formations, such as the triangular septal nucleus and the septofimbrial nucleus (these experiments also labelled sparser neurons within the diagonal band—mainly its horizontal part—and the basal nucleus of Meynert). Work by Swanson and Cowan (1979) and Staines et al. (1988) found in addition habenulopetal neurons within the BAC nucleus, which also targets the rat medial habenula (see also Risold, 2004). We already mentioned results of Watanabe et al. (2018) on habenular projections of calretinin-positive triangular septal nucleus and BAC nucleus in the mouse, which they experimentally proved to migrate from the prethalamic eminence. These migrated septocommissural habenulopetal formations thus correspond clearly to the derivatives of our eminentio-septal migration stream in the chick.

In most cases, these habenulopetal sites are known to contain glutamatergic neurons (Watanabe et al. 2018; Otsu et al. 2018). The habenulopetal hodological similarity of eminential derivatives having quite distinct adult topographies ranging through the PThE itself, peduncular hypothalamus, preoptic area, extended amygdala, diagonal band, posterior commissural septum and BAC, jointly with their general glutamatergic nature, incites the conjecture that these shared properties may be due to a common origin within the prethalamic eminential progenitor domain and its unique molecular specification. The observed hodological groupings with regard to medial versus lateral habenular targets suggests that there might exist separate eminential compartments where these are differentially originated and migrate from; it is revealing that those projecting to the relatively late-born medial habenula neurons seem to migrate selectively through the later developed deep eminentio-septal stream, while those targeting the early-born lateral habenula neurons migrate precociously via the marginal and intermediate peripeduncular and juxtapeduncular streams. It seems also conceivable that all these populations initiate their respective axonal connections with the habenula before they exit the PThE. The causes of their apparent differential migratory behaviour are presently unclear, but a hypothetic single repelling mechanism with the source located at the zona limitans (the mid-diencephalic organizer; Puelles 2017, 2018), or within the habenular area, seems parsimonious compared to the notion of multiple attraction mechanisms. It seems significant that the three streams depart in the same general direction: rostralwards. Maybe the repelled cells just use the nearest available permissive pathways to evade from the PThE at the moment when they are ready to migrate (e.g., after sending out their habenulopetal axons, probably at different time points), thus variously finding by temporal order different target sites.

Acknowledgements We thank F. Marín for critical reading of this manuscript. This work was funded by SENECA contract 19904/GERM/15 to LP.

Compliance with ethical standards

Conflict of interest The authors state that no conflict of interest is involved in the present publication.

References

Abbott LC, Jacobowitz DM (1999) Developmental expression of calretinin-immunoreactivity in the thalamic eminence of the fetal mouse. Int J Dev Neurosci 17:331–345. https://doi.org/10.1016/S0736-5748(99)00037-4

Abellan A, Menuet A, Dehay C, Medina L, Rétaux S (2010) Differential expression of LIM-homeodomain factors in Cajal–Retzius cells of primates, rodents, and birds. Cereb Cortex 20:1788–1798. https://doi.org/10.1093/cercor/bhp242

Abellán A, Medina L (2008) Expression of cLhx6 and cLhx7/8 suggests a pallido-pedunculo-preoptic origin for the lateral and medial parts of the avian bed nucleus of the stria terminalis. Brain Res Bull 75:299–304. https://doi.org/10.1016/j.brainresbull.2007.10.034

Abellán A, Medina L (2009) Subdivisions and derivatives of the chicken subpallium based on expression of LIM and other regulatory genes and markers of neuron subpopulations during development. J Comp Neurol 515:465–501. https://doi.org/10.1002/cne.22083

Abellán A, Vernier B, Rétaux S, Medina L (2010) Similarities and differences in the forebrain expression of Lhx1 and Lhx5 between chicken and mouse: Insights for understanding telencephalic development and evolution. J Comp Neurol 518:3512–3528. https://doi.org/10.1002/cne.22410

Alonso G, Szafarczyk A, Assenmacher I (1986) Radioautographic evidence that axons from the area of supraoptic nuclei in the

rat project to extrahypothalamic brain regions. Neurosci Lett 66:251–256
Barber M, Pierani A (2016) Tangential migration of glutamatergic neurons and cortical patterning during development: lessons from Cajal–Retzius cells. Dev Neurobiol 76:847–881. https://doi.org/10.1002/dneu.22363
Bardet SM (2007) Organización morfológica y citogenética del hipotálamo del pollo sobre base de mapas moleculares. PhD in Biology (Neuroscience Program). University of Murcia, Spain
Bardet SM, Martinez-de-la-Torre M, Northcutt RG, Rubenstein JL, Puelles L (2008) Conserved pattern of OTP-positive cells in the paraventricular nucleus and other hypothalamic sites of tetrapods. Brain Res Bull 75:231–235. https://doi.org/10.1016/j.brainresbull.2007.10.037
Bielle F, Griveau A, Narboux-Nême N, Vigneau S, Sigrist M, Arber S, Wassef M, Pierani A (2005) Multiple origins of Cajal–Retzius cells at the borders of the developing pallium. Nat Neurosci 8:1002. https://doi.org/10.1038/nn1511
Borello U, Pierani A (2010) Patterning the cerebral cortex: traveling with morphogens. Curr Opin Genet Dev 20:408–415. https://doi.org/10.1016/j.gde.2010.05.003
Bulfone A, Puelles L, Porteus MH, Frohman MA, Martin GR, Rubenstein JL (1993) Spatially restricted expression of Dlx-1, Dlx-2 (Tes-1), Gbx-2, and Wnt-3 in the embryonic day 12.5 mouse forebrain defines potential transverse and longitudinal segmental boundaries. J Neurosci 13:3155–3172
Bulfone A, Smiga SM, Shimamura K, Peterson A, Puelles L, Rubenstein JL (1995) T-Brain-1: a homolog of Brachyury whose expression defines molecularly distinct domains within the cerebral cortex. Neuron 15:63–78. https://doi.org/10.1016/0896-6273(95)90065-9
Bulfone A, Martinez S, Marigo V, Campanella M, Basile A, Quaderi N, Gattuso C, Rubenstein JL, Ballabio A (1999) Expression pattern of the Tbr2 (Eomesodermin) gene during mouse and chick brain development. Mech Dev 4:133–138. https://doi.org/10.1016/S0925-4773(99)00053-2
Cabrera-Socorro A, Hernandez-Acosta NC, Gonzalez-Gomez M, Meyer G (2007) Comparative aspects of p73 and Reelin expression in Cajal–Retzius cells and the cortical hem in lizard, mouse and human. Brain Res 1132:59–70. https://doi.org/10.1016/j.brainres.2006.11.015
Carter DA, Fibiger HC (1978) The projections of the entopeduncular nucleus and globus pallidus in rat as demonstrated by autoradiography and horseradish peroxidase histochemistry. J Comp Neurol 177:113–123. https://doi.org/10.1002/cne.901770108
Cobos I, Shimamura K, Rubenstein JLR, Martínez S, Puelles L (2001) Fate map of the avian anterior forebrain at the four-somite stage, based on the analysis of quail–chick chimeras. Dev Biol 239:46–67. https://doi.org/10.1006/dbio.2001.0423
de Olmos JS, Heimer L (1999) The concepts of the ventral striatopallidal system and extended amygdala. Ann N Y Acad Sci 877:1–32
Díaz C, Puelles L (1992a) Afferent connections of the habenular complex in the lizard Gallotia galloti. Brain Behav Evol 39:312–324. https://doi.org/10.1159/000114128
Díaz C, Puelles L (1992b) In vitro HRP-labeling of the fasciculus retroflexus in the lizard Gallotia galloti. Brain Behav Evol 39:305–311
El Mestikawy S, Wallén-Mackenzie A, Fortin GM, Descarries L, Trudeau LE (2011) From glutamate co-release to vesicular synergy: vesicular glutamate transporters. Nat Rev Neurosci 124:204–216. https://doi.org/10.1038/nrn2969
Englund C, Fink A, Lau C, Pham D, Daza RA, Bulfone A, Kowalczyk T, Hevner RF (2005) Pax6, Tbr2, and Tbr1 are expressed sequentially by radial glia, intermediate progenitor cells, and postmitotic neurons in developing neocortex. J Neurosci 25:247–251. https://doi.org/10.1523/JNEUROSCI.2899-04.2005
Fan C-M, Kuwana E, Bulfone A, Fletcher CF, Copeland NG, Jenkins NA, Crews S, Martinez S, Puelles L, Rubenstein JL, Tessier-Lavigne M (1996) Expression patterns of two murine homologs of drosophila single-minded suggest possible roles in embryonic patterning and in the pathogenesis of Down syndrome. Mol Cell Neurosci 7:1–16. https://doi.org/10.1006/mcne.1996.0001
Ferrán JL, Ayad A, Merchán P, Morales-Delgado N, Sánchez-Arrones L, Alonso A, Sandoval JE, Bardet SM, Corral-San-Miguel R, Sánchez-Guardado LO, Hidalgo-Sánchez M, Martínez-de-la-Torre M, Puelles L (2015) Exploring brain genoarchitecture by single and double chromogenic in situ hybridization (ISH) and immunohistochemistry (IHC) on cryostat, paraffin, or floating sections. In: Hauptmann G (ed) In situ hybridization methods, neuromethods, vol 99. Springer Science + Business Media, New York, pp 83–107. https://doi.org/10.1007/978-1-4939-2303-8_5
Fink AJ, Englund C, Daza RA, Pham D, Lau C, Nivison M, Kowalczyk T, Hevner RF (2006) Development of the deep cerebellar nuclei: transcription factors and cell migration from the rhombic lip. J Neurosci 26:3066–3076. https://doi.org/10.1523/JNEUROSCI.5203-05.2006
Font C, Lanuza E, Martínez-Marcos A, Hoogland PV, Martínez-García F (1998) Septal complex of the telencephalon of lizards: III. Efferent connections and general discussion. J Comp Neurol 401:525–548
García-López M, Abellán A, Legaz I, Rubenstein JL, Puelles L, Medina L (2008) Histogenetic compartments of the mouse centromedial and extended amygdala based on gene expression patterns during development. J Comp Neurol 506:46–74. https://doi.org/10.1002/cne.21524
García-Moreno F, Pedraza M, Di Giovannantonio LG, Di Salvio M, López-Mascaraque L, Simeone A, De Carlos JA (2010) A neuronal migratory pathway crossing from diencephalon to telencephalon populates amygdala nuclei. Nat Neurosci 13:680–689. https://doi.org/10.1038/nn.2556
Goodson JL, Evans AK, Lindberg L (2004) Chemoarchitectonic subdivisions of the songbird septum and a comparative overview of septum chemical anatomy in jawed vertebrates. J Comp Neurol 473:293–314. https://doi.org/10.1002/cne.20061
Griveau A, Borello U, Causeret F, Tissir F, Boggetto N, Karaz S, Pierani A (2010) A novel role for dbx1-derived Cajal–Retzius cells in early regionalization of the cerebral cortical neuroepithelium. PLoS Biol 8:e1000440. https://doi.org/10.1371/journal.pbio.1000440
Grove EA, Tole S, Limon J, Yip L, Ragsdale CW (1998) The hem of the embryonic cerebral cortex is defined by the expression of multiple Wnt genes and is compromised in Gli3-deficient mice. Development 125:2315–2325
Hamburger V, Hamilton HL (1951) A series of normal stages in the development of the chick embryo. J Morphol 88:49–92
Hatini V, Tao W, Lai E (1994) Expression of winged helix genes, BF-1 and BF-2, define adjacent domains within the developing forebrain and retina. J Neurobiol 25:1293–1309. https://doi.org/10.1002/neu.480251010
Herkenham M, Nauta WJ (1977) Afferent connections of the habenular nuclei in the rat. A horseradish peroxidase study, with a note on the fiber-of-passage problem. J Comp Neurol 173:123–146. https://doi.org/10.1002/cne.901730107
Hetzel W (1974) Die Ontogenese des Telencephalons bei Lcerta sicula (Rafinesque), mit besonderer Berücksichtigung der pallialen Entwicklung. Zool Beitr 20:361–458
Hetzel W (1975) Der nucleus commissurae pallii posterioris bei Lacerta sicula (Rafinesque) und seine ontogenetische Verbindung zum Thalamus. Acta Anat 91:539–551
Huilgol D, Udin S, Shimogori T, Saha B, Roy A, Aizawa S, Hevner RF, Meyer G, Ohshima T, Pleasure SJ, Zhao Y, Tole S (2013) Dual origins of the mammalian accessory olfactory bulb

revealed by an evolutionarily conserved migratory stream. Nat Neurosci 16:157–165. https://doi.org/10.1038/nn.3297
Imayoshi I, Shimogori T, Ohtsuka T, Kageyama R (2008) Hes genes and neurogenin regulate non-neural versus neural fate specification in the dorsal telencephalic midline. Development 135:2531–2541. https://doi.org/10.1242/dev.021535
Johnston JB (1909) The morphology of the forebrain vesicles in vertebrates. J Comp Neurol 19:457–539. https://doi.org/10.1002/cne.920190502
Kuhlenbeck H (1973) The central nervous system of vertebrates. vol 3, Part II: overall morphologic pattern. S. Karger, Basel
Kumamoto T, Hanashima C (2017) Evolutionary conservation and conversion of Foxg1 function in brain development. Dev Growth Differ 59:258–269. https://doi.org/10.1111/dgd.12367
Louvi A, Yoshida M, Grove EA (2007) The derivatives of the Wnt3a lineage in the central nervous system. J Comp Neurol 504:550–569. https://doi.org/10.1002/cne.21461
Medina L, Abellán A (2012) Subpallial structures. In: Watson C, Paxinos G, Puelles L (eds) The mouse nervous system. Elsevier, Amsterdam, pp 173–220
Meyer G (2010) Building a human cortex: the evolutionary differentiation of Cajal–Retzius cells and the cortical hem. J Anat 217:334–343. https://doi.org/10.1111/j.1469-7580.2010.01266.x
Meyer G, Goffinet AM (1998) Prenatal development of reelin-immunoreactive neurons in the human neocortex. J Comp Neurol 397:29–40. https://doi.org/10.1002/(SICI)1096-9861(19980720)397:1%3c29:AID-CNE3%3e3.0.CO;2-K
Meyer G, Wahle P (1999) The paleocortical ventricle is the origin of reelin-expressing neurons in the marginal zone of the foetal human neocortex. Eur J Neurosci 11:3937–3944. https://doi.org/10.1046/j.1460-9568.1999.00818.x
Meyer G, Goffinet AM, Fairén A (1999) What is a Cajal–Retzius cell? A reassessment of a classical cell type based on recent observations in the developing neocortex. Cereb Cortex 9:765–775
Meyer G, Perez-Garcia CG, Abraham H, Caput D (2002) Expression of p73 and reelin in the developing human cortex. J Neurosci 22:4973–4986. https://doi.org/10.1523/JNEUROSCI.22-12-04973.2002
Morales-Delgado N, Merchan P, Bardet SM, Ferrán JL, Puelles L, Díaz C (2011) Topography of somatostatin gene expression relative to molecular progenitor domains during ontogeny of the mouse hypothalamus. Front Neuroanat 5:10. https://doi.org/10.3389/fnana.2011.00010
Morales-Delgado N, Castro-Robles B, Ferrán JL, Martinez-de-la-Torre M, Puelles L, Díaz C (2014) Regionalized differentiation of CRH, TRH, and GHRH peptidergic neurons in the mouse hypothalamus. Brain Struct Funct 219:1083–1111. https://doi.org/10.1007/s00429-013-0554-2
Namboodiri VMK, Rodriguez-Romaguera J, Stuber GD (2016) The habenula. Curr Biol 26:R873–R877. https://doi.org/10.1016/j.cub.2016.08.051
Nauta HJ (1974) Evidence of a pallidohabenular pathway in the cat. J Comp Neurol 156:19–27. https://doi.org/10.1002/cne.901560103
Nieuwenhuys R, Puelles L (2016) Towards a new neuromorphology. Springer, Berlin. https://doi.org/10.1007/978-3-319-25693-1
Otsu Y, Lecca S, Pietrajtis K, Rousseau CV, Marcaggi P, Dugué GP, Mailhes-Hamon C, Mameli M, Diana MA (2018) Functional principles of posterior septal inputs to the medial habenula. Cell Rep 22:693–705. https://doi.org/10.1016/j.celrep.2017.12.064
Parent A (1979) Identification of the pallidal and peripallidal cells projecting to the habenula in monkey. Neurosci Lett 15:159–164
Parent A (1986) Comparative neurobiology of the basal ganglia. Wiley, New York
Parent A, De Bellefeuille L (1982) Organization of efferent projections from the internal segment of globus pallidus in primate as revealed by fluorescence retrograde labeling method. Brain Res 245:201–213
Parent A, Gravel S, Boucher R (1981) The origin of forebrain afferents to the habenula in rat, cat and monkey. Brain Res Bull 6:23–38
Parent A, De Bellefeuille L, Mackey A (1984) Organization of primate internal pallidum as revealed by fluorescent retrograde tracing of its efferent projections. Adv Neurol 40:15–20
Pattabiraman K, Golonzhka O, Lindtner S, Nord AS, Taher L, Hoch R, Silberberg SN, Zhang D, Chen B, Zeng H, Pennacchio LA, Puelles L, Visel A, Rubenstein JL (2014) Transcriptional regulation of enhancers active in protodomains of the developing cereb cortex. Neuron 82:989–1003. https://doi.org/10.1016/j.neuron.2014.04.014
Paxinos G, Watson C (2014) The rat brain in stereotaxic coordinates, 7th edn. Academic Press, San Diego
Pierani A, Wassef M (2009) Cerebral cortex development: from progenitors patterning to neocortical size during evolution. Dev Growth Differ 51:325–342. https://doi.org/10.1111/j.1440-169X.2009.01095.x
Pombal MA, Puelles L (1999) Prosomeric map of the lamprey forebrain based on calretinin immunocytochemistry, Nissl stain, and ancillary markers. J Comp Neurol 414:391–422
Puelles L (2011) Pallio-pallial tangential migrations and growth signaling: new scenario for cortical evolution? Brain Behav Evol 78:108–127. https://doi.org/10.1159/000327905
Puelles L (2017) Forebrain development in vertebrates: the evolutionary role of secondary organizers. In: Shepherd SV (ed) The wiley handbook of evolutionary neuroscience. Wiley, Chichester, pp 350–387
Puelles L (2018) Developmental studies of avian brain organization. Int J Dev Biol 62:207–224. https://doi.org/10.1387/ijdb.170279LP
Puelles L (2019) Survey of midbrain, diencephalon, and hypothalamus neuroanatomic terms whose prosomeric definition conflicts with columnar tradition. Front Neuroanat 13:20. https://doi.org/10.3389/fnana.2019.00020
Puelles L, Martinez S (2013) Patterning of the diencephalon. In: Rubenstein JLR, Rakic P (eds) Comprehensive developmental neuroscience: patterning and cell type specification in the developing CNS and PNS. Academic Press, Amsterdam, pp 151–172
Puelles L, Rubenstein JLR (2003) Forebrain gene expression domains and the evolving prosomeric model. Trends Neurosci 26:469–476. https://doi.org/10.1016/S0166-2236(03)00234-0
Puelles L, Rubenstein JLR (2015) A new scenario of hypothalamic organization: rationale of new hypotheses introduced in the updated prosomeric model. Front Neuroanat 9:27. https://doi.org/10.3389/fnana.2015.00027
Puelles L, Kuwana E, Puelles E, Bulfone A, Shimamura K, Keleher J, Smiga S, Rubenstein JL (2000) Pallial and subpallial derivatives in the embryonic chick and mouse telencephalon, traced by the expression of the genes Dlx-2, Emx-1, Nkx-2.1, Pax-6, and Tbr-1. J Comp Neurol 424:409–438. https://doi.org/10.1002/1096-9861(20000828)424:3%3c409:AID-CNE3%3e3.0.CO;2-7
Puelles L, Martinez-de-la-Torre M, Paxinos G, Watson C, Martínez S (2007) The chick brain in stereotaxic coordinates: an atlas featuring neuromeric subdivisions and mammalian homologies, 1st edn. Academic Press, London
Puelles L, Martinez-de-la-Torre M, Bardet S, Rubenstein JLR (2012) Hypothalamus. In: Watson C, Paxinos G, Puelles L (eds) The mouse nervous system. Elsevier, Amsterdan, pp 221–312
Puelles L, Harrison M, Paxinos G, Watson C (2013) A developmental ontology for the mammalian brain based on the prosomeric model. Trends Neurosci 36:570–578. https://doi.org/10.1016/j.tins.2013.06.004
Puelles L, Morales-Delgado N, Merchán P, Castro-Robles B, Martínez-de-la-Torre M, Díaz C, Ferran JL (2016a) Radial and tangential migration of telencephalic somatostatin neurons originated from

the mouse diagonal area. Brain Struct Funct 221:3027–3065. https://doi.org/10.1007/s00429-015-1086-8

Puelles L, Medina L, Borello U et al (2016b) Radial derivatives of the mouse ventral pallium traced with Dbx1-LacZ reporters. J Chem Neuroanat 75:2–19. https://doi.org/10.1016/j.jchemneu.2015.10.011

Puelles L, Martinez-de-la-Torre M, Paxinos G, Watson C, Martínez S (2019) The chick brain in stereotaxic coordinates: an atlas featuring neuromeric subdivisions and mammalian homologies, 2nd edn. Academic Press, London

Remedios R, Huilgol D, Saha B, Hari P, Bhatnagar L, Kowalczyk T, Hevner RF, Suda Y, Aizawa S, Ohshima T, Stoykova A, Tole S (2007) A stream of cells migrating from the caudal telencephalon reveals a link between the amygdala and neocortex. Nat Neurosci 10:1141–1150. https://doi.org/10.1038/nn1955

Rendahl H (1924) Embryologische und morphologische Studien über das Zwischenhirn beim Huhn. Acta Zool 5:241–344. https://doi.org/10.1111/j.1463-6395.1924.tb00169.x

Risold PY (2004) The septal region. In: Paxinos G (ed) The rat nervous system, 3rd edn. Elsevier-Academic Press, Amsterdam, pp 605–632

Ruiz-Reig N, Studer M (2017) Rostro-caudal and caudo-rostral migrations in the telencephalon: going forward or backward? Front Neurosci. https://doi.org/10.3389/fnins.2017.00692

Ruiz-Reig N, Andrés B, Huilgol D, Grove EA, Tissir F, Tole S, Theil T, Herrera E, Fairén A (2016) Lateral thalamic eminence: a novel origin for mGluR1/Lot cells. Cereb Cortex 27(5):2841–2856. https://doi.org/10.1093/cercor/bhw126

Ruiz-Reig N, Andres B, Lamonerie T, Theil T, Fairén A, Studer M (2018) The caudo-ventral pallium is a novel pallial domain expressing Gdf10 and generating Ebf3-positive neurons of the medial amygdala. Brain Struct Funct 223:3279–3295. https://doi.org/10.1007/s00429-018-1687-0

Shimogori T, Lee DA, Miranda-Angulo A, Yang Y, Wang H, Jiang L, Yoshida AC, Kataoka A, Mashiko H, Avetisyan M, Qi L, Qian J (2010) A genomic atlas of mouse hypothalamic development. Nat Neurosci 13:767–775. https://doi.org/10.1038/nn.2545

Silberberg SN, Taher L, Lindtner S, Sandberg M, Nord AS, Vogt D, Mckinsey GL, Hoch R, Pattabiraman K, Zhang D, Ferran JL, Rajkovic A, Golonzhka O, Kim C, Zeng H, Puelles L, Visel A, Rubenstein JLR (2016) Subpallial enhancer transgenic lines: a data and tool resource to study transcriptional regulation of GABAergic cell fate. Neuron 92:59–74. https://doi.org/10.1016/j.neuron.2016.09.027

Soriano E, del Río JA (2005) The cells of Cajal–Retzius: still a mystery one century after. Neuron 46:389–394. https://doi.org/10.1016/j.neuron.2005.04.019

Staines WA, Yamamoto T, Dewar KM et al (1988) Distribution, morphology and habenular projections of adenosine deaminase-containing neurons in the septal area of rat. Brain Res 455:72–87

Striedter GF, Marchant TA, Beydler S (1998) The "neostriatum" develops as part of the lateral pallium in birds. J Neurosci 18:5839–5849. https://doi.org/10.1523/JNEUROSCI.18-15-05839.1998

Swanson LW, Cowan WM (1979) The connections of the septal region in the rat. J Comp Neurol 186:621–655. https://doi.org/10.1002/cne.901860408

Takiguchi-Hayashi K, Sekiguchi M, Ashigaki S, Takamatsu M, Hasegawa H, Suzuki-Migishima R, Yokoyama M, Nakanishi S, Tanabe Y (2004) Generation of reelin-positive marginal zone cells from the caudomedial wall of telencephalic vesicles. J Neurosci 24:2286–2295. https://doi.org/10.1523/JNEUROSCI.4671-03.2004

Teissier A, Griveau A, Vigier L, Piolot T, Borello U, Pierani A (2010) A novel transient glutamatergic population migrating from the pallial–subpallial boundary contributes to neocortical development. J Neurosci 30:10563–10574. https://doi.org/10.1523/JNEUROSCI.0776-10.2010

Tissir F, Ravni A, Achouri Y, Riethmacher D, Meyer G, Goffinet AM (2009) DeltaNp73 regulates neuronal survival in vivo. PNAS 106:16871–16876. https://doi.org/10.1073/pnas.0903191106

van der Kooy D, Carter DA (1981) The organization of the efferent projections and striatal afferents of the entopeduncular nucleus and adjacent areas in the rat. Brain Res 211:15–36

Vicario A, Mendoza E, Abellán A, Scharff C, Medina L (2017) Genoarchitecture of the extended amygdala in zebra finch, and expression of FoxP2 in cell corridors of different genetic profile. Brain Struct Funct 222:481–514. https://doi.org/10.1007/s00429-016-1229-6

Wallace ML, Saunders A, Huang KW, Philson AC, Goldman M, Macosko EZ, McCarroll SA, Sabatini BL (2017) Genetically distinct parallel pathways in the entopeduncular nucleus for limbic and sensorimotor output of the basal ganglia. Neuron 941:138–152.e5. https://doi.org/10.1016/j.neuron.2017.03.017

Watanabe K, Irie K, Hanashima C, Takebayashi H, Sato N (2018) Diencephalic progenitors contribute to the posterior septum through rostral migration along the hippocampal axonal pathway. Sci Rep 8:11728. https://doi.org/10.1038/s41598-018-30020-9

Xuan S, Baptista CA, Balas G, Tao W, Soares VC, Lai E (1995) Winged helix transcription factor BF-1 is essential for the development of the cerebral hemispheres. Neuron 14:1141–1152. https://doi.org/10.1016/0896-6273(95)90262-7

Yoshida M, Assimacopoulos S, Jones KR, Grove EA (2006) Massive loss of Cajal–Retzius cells does not disrupt neocortical layer order. Development 133:537–545. https://doi.org/10.1242/dev.02209

Zahm DS, Root DH (2017) Review of the cytology and connections of the lateral habenula, an avatar of adaptive behaving. Pharmacol Biochem Behav 162:3–21. https://doi.org/10.1016/j.pbb.2017.06.004

Zecevic N, Rakic P (2001) Development of layer I neurons in the primate cerebral cortex. J Neurosci 21:5607–5619. https://doi.org/10.1523/JNEUROSCI.21-15-05607.2001

Zimmer C, Lee J, Griveau A, Arber S, Pierani A, Garel S, Guillemot F (2010) Role of Fgf8 signalling in the specification of rostral Cajal–Retzius cells. Development 137:293–302. https://doi.org/10.1242/dev.041178